PREPARATION OF POLYMER MULTILAYER FILMS FOR FOOD TECHNOLOGY APPLICATIONS

A THESIS SUBMITTED TO
THE GRADUATE SCHOOL OF NATURAL AND APPLIED SCIENCES
OF
MIDDLE EAST TECHNICAL UNIVERSITY

BY

GÖKÇE TİDİM

IN PARTIAL FULFILLMENT OF THE REQUIREMENTS
FOR
THE DEGREE OF MASTER OF SCIENCE
IN
CHEMISTRY

JANUARY 2023

Approval of the thesis:

PREPARATION OF POLYMER MULTILAYER FILMS FOR FOOD TECHNOLOGY APPLICATIONS

submitted by **GÖKÇE TİDİM** in partial fulfillment of the requirements for the degree of **Master of Science** i**n Chemistry, Middle East Technical University** by,

Prof. Dr. Halil Kalıpçılar
Dean, Graduate School of **Natural and Applied Sciences** _____

Prof. Dr. Özdemir Doğan
Head of the Department, **Chemistry** _____

Prof. Dr. İrem Erel Göktepe
Supervisor, **Chemistry, METU** _____

Prof. Dr. Yeşim Soyer Küçükşenel
Co-Supervisor, **Food Engineering, METU** _____

Examining Committee Members:

Prof. Dr. Ali Çırpan
Chemistry, METU _____

Prof. Dr. İrem Erel Göktepe
Chemistry, METU _____

Prof. Dr. Yeşim Soyer Küçükşenel
Food Engineering, METU _____

Assoc. Prof. Dr. Özgül Persil Çetinkol
Chemistry, METU _____

Assoc. Prof. Dr. Aylin Üsküdar Güçlü
Clinical Microbiology, Başkent University _____

Date: 20.01.2023

I hereby declare that all information in this document has been obtained and presented in accordance with academic rules and ethical conduct. I also declare that, as required by these rules and conduct, I have fully cited and referenced all material and results that are not original to this work.

Name Last name: Gökçe Tidim

Signature

ABSTRACT

PREPARATION OF POLYMER MULTILAYER FILMS FOR FOOD TECHNOLOGY APPLICATIONS

Tidim, Gökçe

Master of Science, Chemistry

Supervisor: Prof. Dr. İrem Erel Göktepe

Co-Supervisor: Prof. Dr. Yeşim Soyer Küçükşenel

January 2023, 76 pages

In recent years, there has been intense research going on to develop new packaging technologies to improve the safety and quality of the food. Natural polymers not only reduce the consumer health risks but also provide less processed and more environment friendly food packages. Alginate and chitosan are suitable polymers for food technology due to their biocompatibility, biodegradability, and non-toxicity. In addition to the antibacterial properties of chitosan, pH responsive behaviour of alginate and chitosan makes them promising materials for encapsulation and controlled release of functional molecules from surfaces. On the other hand, due to

intensive usage of antibiotic drugs, scientists are in the search of substitute strategies. Bacteriophages are strong candidates for this purpose due to being natural predators of bacteria.

In this thesis study, multilayer films of alginate (ALG) and Chitosan (CHI) were prepared through layer-by-layer (LbL) self-assembly technique. Multilayers were characterized with respect to physicochemical properties such as growth profile, stability, and surface morphology. The drying process between each layer deposition during LbL assembly was found to be critical on the multilayer growth profile. Multilayers which were dried only at the end of LbL process showed exponential growth profile, whereas CHI/ALG multilayers which were prepared by applying a drying procedure after each layer deposition displayed linear growth profile. Multilayers which were not exposed to drying process between the layer depositions were preferred for phage loading studies due to higher film thickness, rough surface morphology, and practicality in preparation. Multilayers were found to be stable at both acidic and neutral pH conditions. The roughness of multilayers increased remarkably as the layer number increased. Bacteriophages, termed T4, which show infection activity towards *Salmonella enterica* subsp. *enterica* serovar Enteritidis were loaded into the films. The effects of layer number, loading pH and release pH on the antibacterial activity of bacteriophage loaded multilayers have been investigated. The pH at which phages were incorporated into multilayers was also found to be critical on the antibacterial activity of the multilayers. Zone formation was observed when phages were loaded at pH 7.0. In contrast, a clear zone was not formed when phages were incorporated at pH 5.0. The pH was also critical on the antibacterial activity. Phage loaded CHI/ALG multilayers demonstrated antibacterial activity at neutral pH. However, zone formation was not observed at moderately acidic pH conditions.

Finally, several antibacterial agents such as curcumin, thymol, lactic acid, and tannic acid were loaded into ALG/CHI LbL films, and their antibacterial properties were compared with those of phage loaded multilayers . No zone formation was obtained

from disc-diffusion tests with the films containing antibacterial agents, pointing out the efficacy of bacteriophages as promising antibacterial entities.

Keywords: Layer-by-layer, natural biopolymers, bacteriophage, antibacterial activity, food packaging

ÖZ

GIDA TEKNOLOJİLERİ İÇİN ÇOK KATMANLI POLİMER FİLMLERİN HAZIRLANMASI

Tidim, Gökçe

Yüksek Lisans, Kimya

Tez Yöneticisi: Prof. Dr. İrem Erel Göktepe

Ortak Tez Yöneticisi: Prof. Dr. Yeşim Soyer Küçükşenel

Ocak 2023, 76 sayfa

Gıda ambalaj teknolojilerinde gıdanın kalite ve güvenliğini artırmak üzerine son yıllarda yoğun çalışmalar yapılmaktadır. Doğal polimerler kullanılarak hazırlanan ya da kaplanan gıda ambalaj malzemeleri, gerek tüketici sağlığı üzerindeki riskleri azaltmaları gerek ise daha az işlenmiş ve daha çevre dostu gıda ambalajları üretme imkânı vermelerinden ötürü tercih edilmektedir. Aljinat ve kitosan biyo-uyumlu, biyo-bozunabilir ve göreceli olarak düşük toksik özellik göstermelerinden dolayı gıda teknolojisi uygulamaları için uygun polimerlerdir. Kitosanın antibakteriyel özelliğinin yanısıra, hem kitosan hem aljinatin pH duyarlı özellikleri, bu polimer ikilisini işlevsel moleküllerin enkapsülasyon/salım uygulamaları için de cazip

kılmaktadır. Öte yandan antibiyotik ilaçların yaygın kullanımından dolayı bakterilerin direnç kazanması, bilim dünyasını farklı yöntemler aramaya itmiştir. Bakteriyofajlar doğal bakteri avcıları olmalarından ötürü umut vadeden bir alternatif olarak karşımıza çıkmaktadır.

Bu tez çalışmasında, katman-katman kendiliğinden yapılanma yöntemi kullanılarak kitosan/aljinat çok katmanlı filmleri hazırlanmıştır. Çok-katmanlı filmler büyüme profilleri, stabiliteleri ve yüzey morfolojisi gibi fizikokimyasal özelliklerini takip etmek üzere karakterize edilmiştir. Çok-katmanlı filmlerin hazırlanması sırasında her katman arasında uygulanan kurutma sürecinin film büyüme profilini belirlemede önemli bir parametre olduğu sonucuna varılmıştır. Sadece bütün polimer katmanları kaplandıktan sonra kurutulan filmler üstel büyüme trendini takip eden kalınlık artışı gösterirken, her katman birikimi sonrasında kurutulan filmlerin kalınlığı doğrusal artış göstermiştir. Katmanlar arası kurutma işlemi uygulanmayan filmler pratik hazırlık aşaması sağladıkları için tercih edilmiştir. Çok-katmanlı filmlerin asidik ve nötr pH değerlerinde stabil oldukları gözlemlenmiştir. Filmlerin yüzey pürüzlülükleri artan katman sayısıyla dikkat çekici şekilde artış göstermiştir. *Salmonella enterica* subsp. *enterica* serovar Enteritidis karşısında aktivite gösteren T4 fajı filmlerin içine yüklenmiştir. Katman sayısı, bakteriyofaj yükleme ve salım pH değerinin bakteriyofaj yüklü çok-katmanlı filmlerin antibakteriyel aktivitesi üzerindeki etkileri araştırılmıştır. Bakteriyofaj yüklenmiş CHI/ALG filmler nötr pH'ta antibakteriyel etki göstermiştir. Diğer yandan hafifçe asidik ortam koşullarında antibakteriyel etki gözlemlenmemiştir.

Son olarak, kurkumin, timol, laktik asit ve tannik asit gibi bazı antibakteriyel ajanlar çok-katmanlı CHI/ALG film katmanlarının arasına yüklenmiş ve bu filmlerin antibakteriyel özellikleri bakteriyofaj yüklü filmlerle kıyaslanmıştır. Bahsi geçen ajanlarla hazırlanan filmlerin disk-difüzyon deneyi sonucunda bakterisiz alan oluşturmaması bakteriyofajların üstün antibakteriyel etkisini işaret etmektedir.

Anahtar Kelimeler: Katman-katman kendiliğinden yapılanma, doğal biyopolimerler, bakteriyofaj, antibakteriyel, gıda paketleme

To my beloved mother, in memory of my father
and those who lost their lives in the recent series of earthquakes that hit my home,
southeastern Turkiye.

ACKNOWLEDGMENTS

First, I would like to thank my supervisor Prof. Dr. İrem Erel Göktepe for her guidance and support throughout the way. She was the reason that I decided to be a scientist in the chemistry area at METU when I had the chance to attend her talk on undergraduate program presentations. She was the role model for me since then and will be forever. I look up to her for her scientific work ethics, sedulity, dedication and most importantly passion for her work.

I appreciate the guidance of my co-advisor Prof. Dr. Yeşim Soyer. She offered me her valuable time and were available whenever I needed help. She opened the doors of her lab for experiments and most importantly shared her lovely phages which is the core of this thesis project.

I would like to thank Dr. Mustafa Güzel specially. He prepared phages during the whole project and taught me how to conduct the antibacterial experiments. Also, he shared all sources of information on phages; books, articles… He was my scientific companion during the project. I also appreciate the other members of Yeşim Soyer's lab.

I would like to thank my defence committee members; Prof. Dr. Ali Çırpan, Assoc. Prof Dr. Özgül Persil Çetinkol and Assoc. Prof Dr. Aylin Üsküdar Güçlü for their time and valuable comments.

My family especially my mother, Dilek Tidim, is the greatest support in my whole life. I would also thank my brother and his wife Dilkut Tidim and Sezen Gücüş Tidim for the light of my life, Işık, my little nephew.

I would like to my lab members, especially, Dilara Gündoğdu, Umut Aydemir, Esma Uğur, Çağrı Turan. During the pandemic, we were an inseparable team and greatest support to each other. I also would like to thank the younger members of our team, İpek Terzioğlu, Ayşe Güren, Cemre Alemdar, Nermin Cemalgil. I am also grateful to my co-workers from analytical laboratory course; especially research asistant,

Begüm Avcı and our lab technician Eda Gökyapı Durkan for their support. I would like to thank my friends, İrem Kolay and Oğuzhan Albayrak for their presence and support.

This project (TEZ-YL-103-2021-10642) has been financially supported by METU Scientific Research Projects (ODTÜ BAP).

TABLE OF CONTENTS

LIST OF FIGURES

LIST OF SCHEMES

LIST OF ABBREVIATIONS

AFM	Atomic Force Microscopy
ALG	Alginate
CHI	Chitosan
CIP	Ciprofloxacin
CMC	Carboxymethyl cellulose
CUR	Curcumin
DLS	Dynamic Light Scattering
DPA	Double plaque essay
EtOH	Ethanol
HA	Hyaluronic acid
LA	Lactic acid
LB	Luria-Bertani
LbL	Layer-by-layer
MH	Mueller Hinton
PAA	Poly(acrylic acid)
PAAm	Poly(acrylamide)
PAH	Poly(allylamine hydrochloride)
PBS	Phosphate buffered saline
PDADMAC	Poly(diallyl dimethyl ammonium bromide)
PE	Poly(ethylene)
PEG	Poly(ethylene oxide), Poly(ethylene glycol)

PEM	Polyelectrolyte multilayers
PET	Poly(ethylene terephthalate)
PLL	Poly(L-lysine)
PP	Poly(propylene)
PSS	Poly(styrene sulfonate)
PVC	Poly(vinyl chloride)
PVPON	Poly(vinylpyrrolidone)
TA	Tannic acid
TEM	Transmission Electron Microscopy
THY	Thymol
QCM-D	Quartz Crystal Microbalance with Dissipation Monitoring
WHO	World Health Organization

CHAPTER 1

INTRODUCTION

1.1 Food Packaging

Food preservation is greatly ensured by packaging, which surrounds the food in a barrier of protection. Food packaging contributes to the preservation of product quality and safety. Also, it helps to extent the product's shelf life by providing protection against physical, chemical, biological, or environmental damages during transportation and storage [1]. In general, packaging has three main purposes which are to protect the goods, to carry information via providing a printed branding and nutritional information section, and to transport the product safely [2].

Food spoilage is typically caused by oxidation, microbial spoilage and metabolism, which can be influenced by factors such as temperature, humidity, light, physical damage, microorganisms and so on [3]. Food is packaged to maintain its quality, ensure its safety, and increase its shelf-life duration. For example, preserving fruits and vegetables requires reducing respiration and transpiration rate, which is typically accomplished by controlling humidity, temperature, light, and the gas environment (O_2, CO_2, ethylene) [3]. Different categories of foods have different requirements for their storage and transport. In case of dairy products such as milk, cream or cheese, the spoilage is generally caused by oxidation and microbial growth. Therefore, external factors like oxygen, light, and moisture must be carefully considered. Meat products are susceptible to discolouration due to oxidation, which can be avoided by vacuum or modified atmosphere packaging.

1.1.1 Types of Food Packaging

Scientists have been working on developing novel and better packaging technologies every day to increase shelf-life and quality of food during storage. In the recent years, intelligent (smart) and active packaging technologies substituted the conventional food packaging technologies which are termed as passive packaging [4].

1.1.1.1 Passive Packaging

Passive packaging term is generally used for more primitive packaging technologies which only function as an inert barrier between the product and the environment to protect food from negative effects of moisture and oxygen [4].

1.1.1.2 Intelligent/Smart Packaging

Smart or intelligent packaging terms are often used interchangeably. “Smart” word was first used for packaging technologies by Sneller and co-workers in 1986 to describe selectively permeable membranes consisting of polyethylene films which allowed CO_2 to escape from the package and prevent O_2 from entering [5]. Packaging that has an exterior or internal indication to convey details about the package's history or the food's quality is referred as intelligent packaging [6]. Intelligent packaging detects certain characteristics of the food or the environment in which it is stored and can alert the producer, distributor, or customer to the condition of these qualities [7]. Intelligent packaging technologies can inform the consumer about the quality of the food by showing when it is ripe or fresh, or if its shelf life has run out.It can show the temperature of the food using thermochromic inks or microwave doneness indicators, display the temperature history of the food using time–temperature indicators, and show if a package has been altered.

1.1.1.3 Active Packaging

Active (short for interactive) packaging systems increase the functional qualities of food packaging by releasing active agents in a controlled and specific manner or in a nonmigratory manner, acting without migration of any material [8,9]. Active packaging refers to the inclusion of specific additives into package whether loose within the system, affixed to the interior of packaging materials, or included into the packaging materials themselves to preserve or increase product quality and shelf life. Active packaging can be used to remove undesirable compounds such as C_2H_4 produced by respiring fruits or O_2 present inside a package, add a desired compound such as CO_2 or ethanol (to inhibit microbial growth), prevent microbial growth (such as by incorporating an antibacterial chemical into a film), change permeability to gases as the temperature changes and so on. Active packaging is described as packaging technologies in which supplementary ingredients have been purposefully added to, removed from, or otherwise modified the packing material to improve the performance. Active packaging applications include; oxygen, carbon dioxide, ethylene absorbers, ethanol emitters, moisture, flavour, odour adsorbers, self-heating/cooling, changing gas permeability and so on [6].

Active packaging is useful especially in case of antimicrobial packaging applications of food products such as fresh meats because traditional methods to inhibit microbial growth on food like adding antimicrobial agents directly cannot be applied to such products. Antibacterial sprays or dips have been used to increase safety and postpone deterioration since microbial contamination of these items occurs predominantly at the surface because of post-processing handling. However, the benefits of directly applying antibacterial compounds to food surfaces are limited since the active ingredients either neutralize upon contact or disperse quickly into the bulk food. Therefore, antimicrobial packaging particularly become prominent among active and intelligent packaging applications [6].

1.1.1.4 Antimicrobial Packaging

The growing customer demand for minimally processed preservative-free, "fresh" foods is what's boosting interest in antimicrobial food packaging. Antimicrobial food packaging, which can take many different forms, decrease, block, or delay the development of microorganisms that may be present in the packaged food or packaging material. Use of polymers that are naturally antimicrobial, incorporation of volatile and non-volatile antimicrobial agents into polymer matrices, coating or adsorbing antimicrobial agents on polymer surfaces, immobilization of antimicrobial agents to polymers by covalent or ionic bonding and adding sachets or pads containing volatile antimicrobial agents to packages are all examples of antimicrobial packaging methods. Since food deterioration mostly happens on the surface, there is no need to incorporate large quantities of antimicrobial agents into the bulk of the food. When compared to adding preservatives directly to the food, one significant benefit of using antimicrobial packaging is that very little preservative actually contacts the food [9].

To increase shelf life and ensure food safety, antimicrobial packaging materials must decrease the development rate of microorganisms. Ethanol and other alcohols, organic acids and their salts including benzoates, propionates, and sorbates, fungicides like imazalil and benomyl, enzymes as glucose oxidase, lactoperoxidase, and lysozyme, extracts from spices and herbs, SO_2 and ClO_2, silver, and bacteriocins are just a few of the substances that have been tested or proposed as antimicrobial agents. The most common antibacterial agents are; bacteriocins and enzymes (nisin, lysozyme, lactoperoxidase etc.), metal ions (silver, zinc and so on.), nanoparticles, essential oils, extracts (thymol, eugenol, carvacrol, curcumin etc.), organic acids (lactic acid, sorbic acid, benzoic acid, propionic acid etc.), and polymers showing antimicrobial activity such as chitosan. Due to its inherent antimicrobial characteristics and capacity to serve as both a film matrix and a carrier of antimicrobial additives, chitosan has been widely explored as an antimicrobial agent in food packaging [6].

1.2 Bio-based, Edible and Biodegradable Materials for Food Packaging Applications

In the present era, scientists are mostly interested in providing long term preservation without compromising from the quality of food while deadening the environmental concerns arising from extensive plastic pollution [1]. Polymers are the reason of various ecological problems when used as food packaging materials if they do not show biodegradable properties. Approximately 36% of the plastics are used in packaging applications including single use [10]. Reduction of petrochemical based polymers such as, polyethylene terephthalate (PET), polyvinyl chloride (PVC), polyethylene (PE), polypropylene (PP) in packaging applications is desired because they are not completely recyclable and/or biodegradable [11].

Materials for sustainable and biodegradable food packaging that are based on biopolymers have aided the industries in overcoming these difficulties. Bio-based polymers are an outstanding candidate for this purpose because of their properties such as biodegradability, renewability, bioavailability, biocompatibility, and non-toxicity [1,3,10–12]. Moreover, some of the biopolymers are edible, so, they can be used as coating materials directly on the food material. Also, they show good qualifications in terms of mechanical properties and moisture, gas and thermal barrier specialities and result in comparable properties with conventional polymers [9,10,12]. They can be used to design systems that can release active ingredients in a controlled manner. The environmentally friendly biopolymer packaging is frequently used to ensure the safety and quality of meat products [3]. Their most salient disadvantage is expensive manufacturing processes [9]. Additionally, many biodegradable materials, including those based on proteins and polysaccharides, are hydrophilic and extremely crystalline, which can have adverse effects on their mechanical performance especially during processing. Therefore, to provide these bio-based polymers thermoplastic behaviour and make them compatible with plastic processing methods, the structures of these materials must be altered. According to Zhang et al., plasticizers including glycerol, polyethylene glycol, and

sorbitol can be used to boost the performance of the packaging material produced from the proteins obtained from defatted canola meal. The mechanical properties of protein-based biodegradable packaging was increased by reducing brittleness and enhancing flexibility and elasticity [13].

There is an increasing interest in edible coatings as alternative storage materials due to environmental concerns. In addition to being biodegradable and biocompatible by nature, edible coatings and films made of proteins, lipids, and polysaccharides offer barrier qualities against oxygen and physical stress [14]. The purpose of edible packaging is to provide a selective barrier to inhibit moisture migration, gas transfer, oil, and fat migration, and to increase the mechanical properties. Also, there are edible packaging technologies which enhance the food's handling qualities or mechanical integrity; eliminate volatile flavour molecules and contain anti-oxidants and antimicrobial agents [6]. However, the choice of the included active agents is restricted to edible chemicals in the case of edible films and coatings. Their safety is critical since the purpose is to consume the film/coating together with food itself [15].

1.2.1 Chitosan (CHI)

Chitin is the most abundant biopolymer on earth after cellulose. It can be found within the shells of arthropods which includes insects and marine crustaceans, as well as the cell walls of various microorganisms such as several fungi species, bacteria, algae etc, but the main production of chitin is from waste exoskeletons of marine crustaceans such as shrimp, crab and so on [16,17]. However, applications of chitin are not nearly as prevalent as cellulose despite the fact of being highly abundant. The reason of this is the relatively more difficult extraction of chitin from its natural sources. Moreover, acquiring stable chitin solutions are more difficult, and batch-to-batch variation is an important problem, resulting in non-reproducible experimental outcomes. This is because of use of diverse extraction processes leading to variable molecular weights and randomly positioned acetyl groups [18].

Chitin shows low solubility in most organic solvents and water due to high intramolecular interactions established via hydrogen bonding between O(3′)-H hydroxyl to O(5) ring oxygen, causing a rigid linear backbone. Also, *N*-acetyl groups constitute hydrogen bonds in three dimension, which eventually form stacked morphology of chitin [19]. Ideal solvents for dissolving chitin are concentrated acids and amide/LiCl (mixture of LiCl and N,N-dimethylamide) systems. However, these solvents may cause chain degradation. In addition, in case of solvent evaporation, any residue may cause toxic effect for biomedical and food applications [19]. For these reasons, chitin is mostly produced to convert into chitosan and used in this form [18].

Chitosan is obtained via N-deacetylation of chitin (Scheme 1) [3]. Because of glucosamine units, CHI is a soluble polycation in dilute acid solutions below pH 6.0, when degree of deacetylation exceeds 50% [17,19,20].

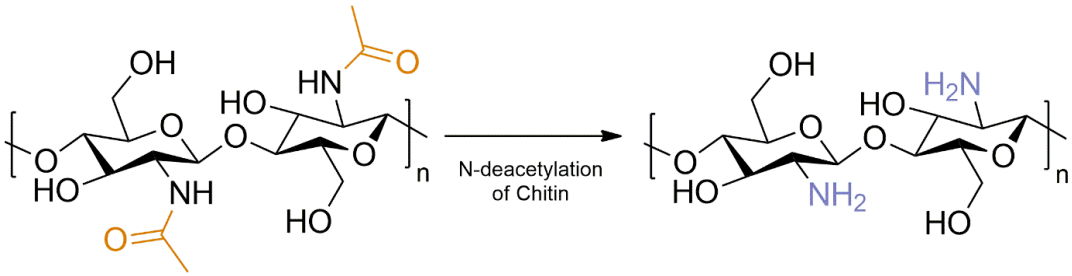

Scheme 1. Chitosan production from chitin via N-deacetylation.

CHI production from chitin was first reported in 1859 by Rouget with alkaline treatment at high temperatures. Currently, mostly this production method is used to get CHI for industrial scale. However, other methods such as biotechnological methods have also been developed [20]. CHI is a popular polymer for antimicrobial active food packaging applications due to being biodegradable and showing antibacterial properties. It has been shown that CHI is effective against both Gram-positive and Gram-negative bacteria and fungi. The chitosan glucosamine monomer has a positive charge at the C-2 position at acidic pH values. The polymer may easily interact with negatively charged microbial cell membranes. This interaction causes proteins and other internal components to leak. Microbial activity is significantly

impacted by charged groups on CHI. Polycationic CHI attaches to the cell surface of a target microorganism and causes agglutination. Additionally, CHI can change the permeability of the baker's yeast cell membrane to block the entry of glucose, which the yeast needs for development. CHI may bind to trace metals to eliminate the toxins created by microbes since it is a powerful chelating agent. CHI can attach to DNA after it enters nuclei, prevent the synthesis of mRNA, and inhibit the production of amino acids [9].

1.2.2 Alginate (ALG)

Since their discovery in the late 19th century, alginate, which is found in brown algae cell walls and is harvested commercially from coastal areas, has grown to be a very important biomaterial. It is obtained from bacterial and algal sources, nowadays commercially obtained from brown algae (*Phaeophyceae*). It is an unbranched polysaccharide consisting of two different repeating units which are β-(1→4)-linked D-mannuronic acid (M) and α-(1→4)-linked L-guluronic acid (G) residues (Scheme 2) [21].

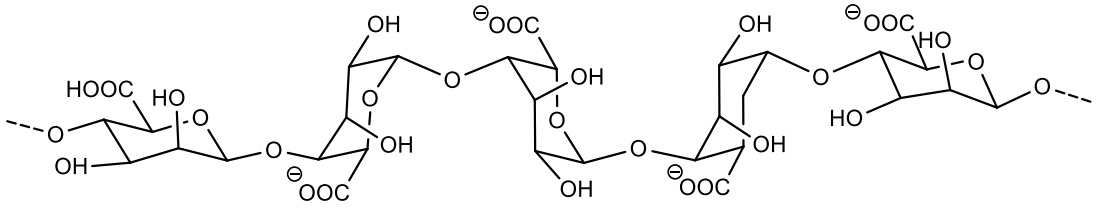

Scheme 2. Alginate structure.

ALG is an indigestible biopolymer. It is in anionic form in a wide pH range (p*K*a values of guluronic acid and mannuronic acids of ALG are around 3.65 and 3.38, respectively) [22]. It is used for various applications in the fields of biotechnology, biomedical applications, medicine, beverages, and the food industry due to being biodegradable, biocompatible, having relatively low toxicity, low production cost and good gelation properties. Also, it is widely used for food and industrial

applications because of high water holding and retaining capacity, stabilizing, emulsifying and viscosifying properties [21].

ALG shines out especially for edible coating/film systems in food packaging applications due to its exquisite film forming and gelation characteristics. Also, properties of ALG containing packaging materials can be improved with various additives. For example, addition of plasticizers can enhance mechanical properties of such packages. Main goals of plasticizers are to increase the free volume of polymers, or their molecular mobility, decrease intermolecular forces, enhance flexibility, reduce brittleness, and improve tear impact resistance [23].

Systems that are constructed with ALG are also susceptible to incorporation with active agents such as antimicrobial or antioxidant molecules. The addition of antimicrobial and antioxidant compounds to coatings and films consisting of ALG offers the chance to gradually release the agents while maintaining a critical concentration for an extended length of time. On the other hand, the direct addition of antimicrobials to food will immediately suppress microbial growth in contrast to the diffusion of antimicrobials from the coating. However, the recovery of damaged cells and the subsequent development of undestroyed cells may result in quality losses and/or foodborne illnesses. There are numerous studies which ALG coating applied on food such as fruits (apple, melon, strawberry, pineapple…), beef, chicken, fish, and cheese. These coatings are enriched *via* incorporation of antimicrobial reagents like oregano, thyme oil, malic acid, carvacrol, *trans*-cinnamaldehyde, pomegranate peel extract, nisin, lactic acid, and lactoperoxidase enzyme [24].

1.3 Bacteriophages and Phage Therapy

Bacteriophages, shortly phages are viruses that naturally predate bacterial cells, known as the deadliest beings around the globe with the estimated total number of 10^{32}. Moreover, there are 10^{9} virions per gram of soil, and 10^{4} to 10^{8} virions per mL

of water in aquatic systems. Every day, up to 40% of the bacteria living in the oceans are killed by bacteriophages [25].

The phages were first discovered separately by British pathologist Frederick William Twort and French-Canadian scientist Félix Hubert d'Hérelle in 1915. However, the studies gained momentum with the developments of electron microscope in 1940s [25] and there are more than 6000 phage species discovered until today [26]. Most of them have icosahedron head structure containing genetic material (mostly double stranded DNA), tail and fiber legs. They can be classified based on their genetic material (double or single stranded DNA/RNA), morphologies (tailed phages, icosahedral phages, filamentous phages) and particular hosts (e.g., the staphylococcal phage family).

Phages have attracted scientists' interest in 2000s mostly due to emergence of antibiotic-resistant bacteria around the globe. Overuse of antibiotics caused bacteria to gain resistance via mutations, and the resistance has been recognized as an health care emergency [26] by Infectious Disease Society of America in 2008 [27]. Bacteriophages and phage therapy are considered as a legitimate alternative to antibiotics since phages are very target-specific, generally can only infect a single species of bacteria or certain bacterial strains in that species.

A phage's capacity to successfully infect a host cell depends on i) its capacity to adhere to the cell, ii) insert its genetic material, iii) prevent that genetic material from degrading while the host cell's replication machinery is switched over. After that, the bacteriophages produce and put together mature virions from the phage's components, and finally lyse (for phage therapy the interest is concentrated on lytic phages mostly [26]), release the newly formed phages to the cell. The host range of the phage excludes this species or strain if any of these processes are prevented by host cell mechanisms or physiology, which prevents the phage from productively infecting the bacterial strain [28]. Therefore, the side effects are minimized and phages cannot harm the beneficious bacteria like unselective antibiotics. Additionally, even when a certain phage may successfully infect a specific bacterial

species or strain, that strain might quickly acquire phage resistance. The resistance may be gained through, for instance, changing or downregulating the phage receptor. However, if the selective pressure caused by the phage's presence is preserved, this new mutant clone will be retained despite its diminished efficiency. This fact is due to mutable nature of the phages. They can adapt the situation just like bacteria. This dynamic adaptation process between phages and bacteria promotes mutations for not only bacteria but also both species simultaneously [28]. Additionally, phages can be used as “phage cocktails” and there are proven cases that when used with antibiotics, they show synergistic effect [27]. Moreover, a very small amount of phages (even in nanograms) show efficient antimicrobial effect due to in situ replication leading to the higher number of phages on the site of action [28].

Phages are already numerous in nature and can be easily isolated. They have low toxicity since they only consist of proteins and genetic material (and occasionally enzymes) [29]. Above all, they are effective against antibiotic-resistant bacteria hence phage resistance and antibiotic resistance are unconnected phenomena. Finally, it is easy to manipulate and modify phages. Hence, therapeutically enhanced phages can be obtained and used in long term [28]. Phage therapy is a promising method against antibiotic-resistant bacteria originated diseases. However, the applications are not limited to that. Phages are used in veterinary purposes, agricultural and industrial applications, clinical studies carried out to be able to identify and characterize bacteria, and finally; food safety [26].

1.3.1 Food Safety Applications of Phages

Worldwide, a wide range of goods with animal and plant origins are purchased and consumed daily with the expectation that they are secure. However, a wide range of foodborne infections cause millions of people to become sick, require hospitalization, and even pass away every year. For instance, the World Health Organization (WHO) projected that over 1.8 million people died from diarrheal infections in 2005 in their information sheet from March 2007 (no. 237).

Additionally, foodborne bacteria are responsible for around 48 million illnesses, 128,000 hospitalizations, and even 3,000 fatalities per year in only the United States [29]. According to data obtained from the WHO, each year, severe foodborne illnesses cause of death of up to 420,000 people, which affect 600 million people worldwide. 30% of the death cases occurred among the children with age less than 5. It is estimated that this would have a financial effect of more than $110 billion owing to the direct expenses of healthcare and the indirect costs caused due to losing productivity [30].

Bacteriophages can be used on farm, to reduce colonization in living animals via mixing in the water that animals consume or oral/injection delivery. They can be used for post-harvest applications such as spraying on the food surfaces, used to sanitize the equipment or food contact surfaces. Additionally, they are used to prevent bacterial spoilage during the storage in the production line, markets, and houses since they show antibacterial activity at even low temperatures (as low as 1 °C). There are reports showing that phages slowed down the growth of bacteria which cause spoilage on refrigerated foods [29].

The research on food safety applications is generally focused on four main animal originated pathogens; *E. coli, Campylobacter, Salmonella,* and *Listeria*. These bacteria are the main contaminants of animals which are subject to food industry and considered as the most dangerous pathogens on food safety scope [29]. The phages used in this thesis study is specific to *Salmonella enterica* serovar Enteritidis which is the number one reason of zootonic diseases around the globe.

1.3.1.1 *Salmonella* Phages for Food Safety Applications

Salmonella serovars cause unpleasant symptoms like diarrhea, fever, abdominal cramps and pain, chills, vomiting, headache and even cause death [31]. Nearly 3 million euros are spent every year in the EU on health care systems due to *Salmonella* infections. Most *Salmonella* outbreaks are believed to be caused by consumption of

infected eggs and chicken, pig, and bovine meats. Of note, even processed meat can cause infections. *Salmonella enterica* serovars Enteritidis and Typhimurium are considered as the main cause of most outbreaks [29].

There are numerous studies on *Salmonella* phage applications for food safety applications. They can be classified as pre- and post-harvest applications mainly. Pre-harvest applications generally include oral delivery (*via* feed and drinking water). There are numerous pre-harvest *Salmonella* phage studies conducted on poultry and swine. Attenbury and co-workers, obtained broiler chickens which they were sure of free of any *Salmonella* infections. They treated the birds with i) *Salmonella* only, ii) phage only and iii) both *Salmonella* and phage. They sacrificed one animal per day up to six days and enumerated the bacteria and phage content from the contents of their cecum. As a result they found that; Φ151, Φ25 phages reduced bacteria concentration 4.2 (*S. enterica* serotype Enteritidis) and 2.19 (*S. enterica* serotype Typhimurium) orders in 24 hours compared to control [32]. There are also post-harvest applications of phageson cheese, fruits, meat, seeds, and ready-to-eat foods. In post-harvest applications, the bacteriophage solution can be applied on food by spraying, immersing or can be added to food directly. For example, Modi and co-workers conducted a study on cheddar cheese made from raw and pasteurized milk containing 10^4 CFU/ml of *Salmonella* Enteritidis and 10^8 PFU/ml bacteriophage. The final amount of *Salmonella* Enteritidis survived in the milk was 10^3 CFU/g. Even after 89 days, they did not observe any presence of bacteria in the cheese produced from pasteurized milk. For the cheese produced with raw milk, final bacteria concentration was found as 50 CFU/g [33]. Other studies such as seeds immersed in phage solution, resulted in reduction in bacteria content by 1.37 logs for mustard seeds and 1.50 logs for broccoli seeds [29]. There are also studies conducted on chicken meat. Whichard and co-workers showed that bacteriophage the Felix O1 supressed *Salmonella* growth between 1.8 and 2.1 log units [34].

1.4 Layer-by-Layer (LbL) Self-Assembly Technique

Layer-by-layer self-assembly technique consists of alternating deposition of interacting polymers onto a substrate surface *via* intermolecular interactions such as electrostatic forces, hydrogen bonding or with directly forming covalent bonds, host-guest interactions [35]. After each layer deposition, substrate should be exposed to a washing step to get rid of weakly attached species onto the surface, hence increasing film stability. Also, rinsing step prevents contamination between the solutions. LbL film deposition is based on sequential deposition of polymer layers one by one, until desired layer number is reached (Scheme 3).

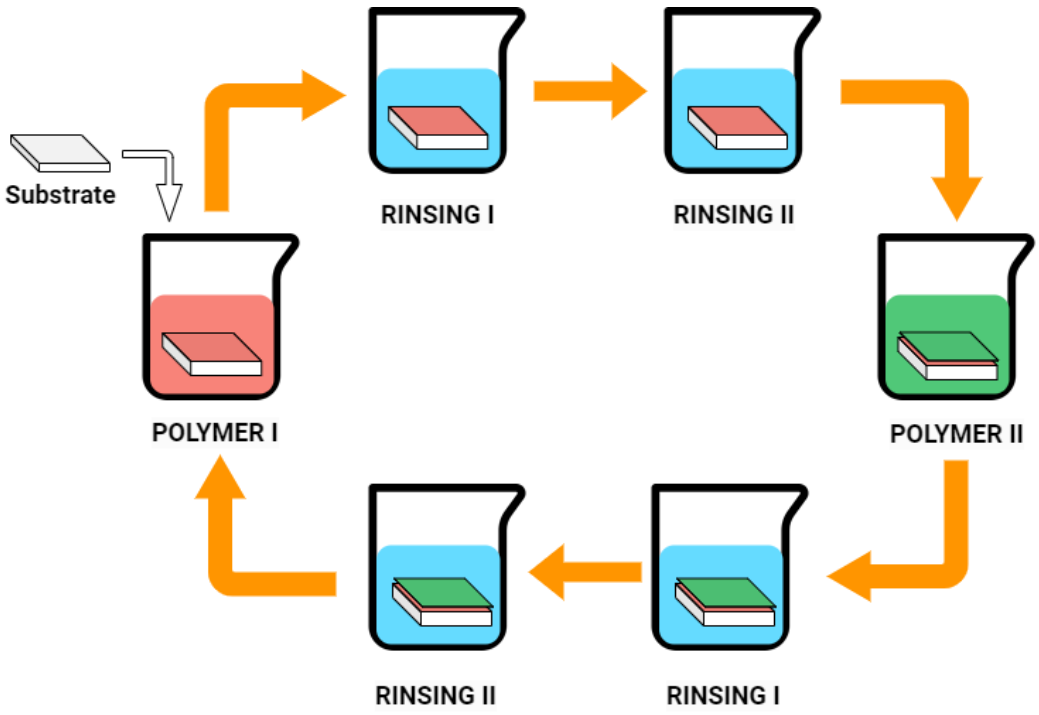

Scheme 3. Layer-by-layer deposition of polymers onto a substrate.

The LbL technique was first introduced by Iler in 1966 [36] through alternating deposition of colloidal alumina and silica particles onto a black plate glass. In 1990s, Decher applied this technique to oppositely charged polyelectrolytes [37] and

described the LbL method for every step in detail; from surface cleaning and functionalization procedure for substrates [38], to LbL film deposition conditions and characterization methods [38–40]. After Decher applied LbL technique to polymers, an increasing attention emerged among scientists to this approach. In the early 2000s, the articles on LbL technique could be counted on the fingers of one hand per year. However, there are more than seven hundred articles published per year in the last decade [41]. This method is used in various areas such as food preservation [13], drug/protein-peptide-hormone/DNA-plasmid delivery, [36], tissue engineering [37], regenerative medicine, biosensor applications [44–47], membrane technologies [48,49], and electrochemical applications [50,51].

LbL assembly is a simple, effective, highly reproducible, robust, and incredibly versatile technique for modifying surfaces and fabricating ordered multilayer thin films and nanocomposites of polymeric molecules. The layer thickness, composition and structure can be controlled. LbL assembly can be carried out in confined environments on virtually any substrate (such as planar, porous, colloidal particles, and cylindrical structures) with almost any surface chemistry. It also enables the incorporation of a wide variety of building blocks into the multilayer, such as polymers, peptides, carbon nanotubes, clays, dyes, metal oxides, and other components like particles, nucleic acids, proteins, enzymes, and viruses. Additionally, the assembly process can be carried out at room temperature, and it is relatively inexpensive (only simple laboratory equipment is needed). It also enables the incorporation of a large variety of biomolecules in the films. It can be carried out under mild conditions, entirely aqueous solutions without exposure to organic solvents or extreme temperatures or pH values. As a result, it is regarded as an environmentally friendly fabrication process. This is a crucial characteristic, especially when working with biomolecules including nucleic acids, polypeptides, polysaccharides, proteins, enzymes, viruses, and even cells, which are prone to denaturation (loss of biological activity) and have a restricted solubility in nonaqueous solutions. This gives a lot of control over the composition of the film

thanks to the ability to alter the type of building blocks that are deposited during each phase [52].

Polymer layers can be deposited onto templates chosen from any flat surfaces or hard and soft colloidal particles [53] like mentioned before. By applying LbL method on the template, one can built a foundation for giving the surface any desired property. For example, drugs can be loaded for biomedical applications or active agents such as antimicrobial molecules encapsulated into the multilayer systems for food packaging applications. LbL approach enables scientists to modify the release pattern of molecules of interest, for example by giving the ability of sustained/controlled release property of therapeutics for smart drug delivery applications. Additionally, when LbL technique is applied for functionalization of colloidal particles. It enhances colloidal stability of coated nano/micro-carriers, increases stability of relevant molecules that are desired to be transmitted without destruction of molecular integrity, improves stability and permeability. Finally, for the purpose of protecting active ingredients and improving colloidal stability, LBL method is applied to a variety of nanocarrier systems, including nanobubbles, nanoporous templates, liposomes, hydrogel, thin films, and nanocapsules [54].

Multilayer assemblies are typically prepared by LbL accumulation through a variety of deposition techniques, including dip-coating, spin-coating, spraying, and perfusion. The dip-coating method of creating multilayers is currently the most popular one. The ability to coat substrates with more complex geometries is a benefit of this technique. However, the other techniques also have their advantages. For example, spray-coating is a good alternative since it is rapid and requires less material for successive layer deposition [52]. The perfusion technique is especially practical for building nanostructured scaffolds from nano-beads and fibers [55]. Spin-coating is advantageous because it significantly reduces LbL assembly time duration[56]. Moreover, since spin-coated films are not strongly bounded to the substrate surface, they can be used to obtain self-standing films [57].

As discussed earlier at the beginning of this section, the driving forces that enable materials to accumulate LbL on any given substrate may be the electrostatic interactions between the components if they have oppositely charged units. However, note that the interactions are not limited to that. Despite of the vast variety of possible interactions, electrostatic attractions and hydrogen bonding are the most common driving forces used in LbL self-assembly.

1.4.1 Layer-By-Layer Assembly Based on Electrostatic Interactions

When a molecule and an adsorbent surface are both electrically charged, the electrostatic contact is one of the most significant, if not the preferred, among the interactions between the molecule and the surface. Moreover, the vast majority of papers in the literature demonstrate that this kind of interaction was the first and is by far the most investigated assembly mechanism within the LbL method [52].

Early research revealed that the fundamental driving force behind the formation of multilayer thin films was the electrostatic interaction between molecules with opposing charges. This notion was accepted after the discovery that a minimum molecular charge density was required for the formation of successful layers. In this case, the adsorption will probably cease when the coated surface has a net neutral charge. In recent years, certain polymers with low charge densities have been successfully produced in multilayer films using the LbL assembly process. This explanation based on a minimal charge density was proven to be insufficient. Then, it has been shown that the formation of multilayer films was not limited to substances that had charged groups. As a result, in addition to electrostatic interactions, other driving interactions such as hydrogen bonding have become a preferable option when constructing multilayer thin films [52].

By simply repeating the alternate immersion of a charged substrate into diluted solutions of oppositely charged polymers (Scheme 4), LbL assembly based on electrostatic interactions enables us to build multilayer films with well-controlled

composition, structure, and thickness. The manufacture of homogenous multilayer ultrathin films from mixed materials is suitable for several uses, including biomedical ones. Despite the increase in LbL assembly-related papers, more thorough knowledge is still needed to completely understand the mechanisms behind recharging and the factors that promote the formation of multilayer films [58].

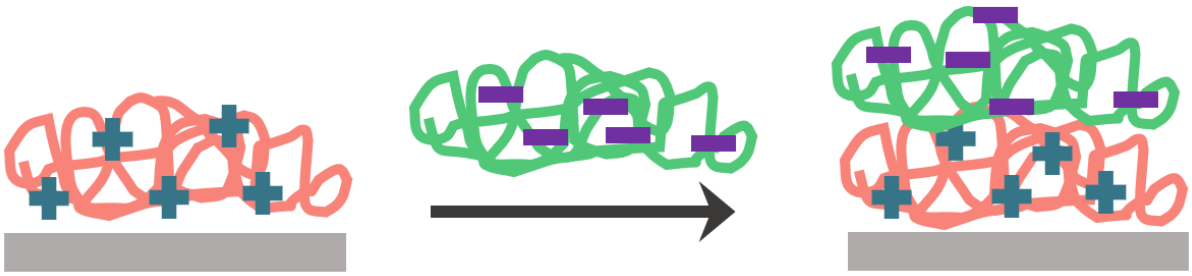

Scheme 4. Sequential deposition of two oppositely charged polyelectrolytes onto a substrate.

1.4.2 Layer-By-Layer Assembly via Hydrogen Bonding

Stockton and Rubner were the first researchers studied LbL assembly based on hydrogen bonding. After a short time period Zhang and co-workers published another study on multilayer deposition of poly(4-vinylpyridine) and poly(acrylic acid) via hydrogen bonding interactions [59,60]. Stockton and Rubner were able to prepare hydrogen-bonded LbL constructed films by alternating deposition of polyaniline and a range of nonionic polymers such as poly-(vinylpyrrolidone) (PVPON), PVA, poly(acrylamide) (PAAm), and poly(ethylene oxide) (PEG). FTIR spectroscopy was used to follow self-assembly of multilayers. Additionally, using ellipsometry and UV-vis spectrophotometry, the effects of solution pH and polymer molecular weight on the deposition process were investigated. It was discovered that both variables had significant impact on the electrical conductivity and bilayer thickness of the multilayer films. Reducing pH caused the bilayer's thickness to rise

for most of their systems (except PEG) [60]. Sukhishvili and Granick also described deposition of multilayers of poly(acrylic acid), poly-(methacrylic acid) and poly(vinylpyrrolidone) and poly(ethylene oxide) through hydrogen bonding interactions. They examined the stability of the films with respect to pH and monitored the release of rhodamine 6G, a dye, from multilayers. They laid the groundwork for release of active reagents such as drugs and antimicrobial agents from hydrogen-bonded multilayer systems [61].

Films that respond to ambient pH and/or temperature at moderate pH levels could be formed using hydrogen bonded LbL assembly. Future uses of such assemblies as pH- and/or temperature-responsive drug delivery materials or release from films were compatible with biological tissues. Using this method, surface-attached hydrogels, or crosslinked capsules, as well as single-component hydrogel materials, were produced. These materials preserve the potential of hydrogen bonded films to respond to environmental stimuli while displaying enhanced stability towards pH changes. Finally, new possible uses for hydrogen bonded LbL films as flexible free-standing films were opened by the possibility of incorporating polymers with low glass transition temperatures, such as poly(ethylene oxide) (PEG) into LBL films. One such prospective use is the proton-exchange membranes for fuel cells or food packaging applications [58].

1.4.3 Parameters Effecting the LbL Growth, Structure, and Properties of Multilayer Assemblies

The architecture and properties of the films deposited by LbL method can be well controlled at the nanometre-scale level. Tuning characteristics of film structure can be possible by adjusting the properties such as the charge density, composition, and structure of the adsorbed species. Also, the properties of the liquid medium, such as the salt/buffer composition, solvent quality, and ionic strength are critical to control film characteristics such as the thickness, stiffness, chemical composition, structure, roughness, wettability, and swelling/shrinking behaviour [33].

1.4.3.1 Effect of pH

The pH value of the polyelectrolyte solution modifies the composition and structure of each layer of coating by altering the charge density and degree of ionization of weak polyelectrolytes. The number of ionized and non-ionized functional groups in weak polyelectrolytes is changed with changing pH, which particularly affects weak polyelectrolytes that include a carboxylic acid or amine group. Additionally, it affects the conformation of the weak polyelectrolytes within the multilayers as well as the swelling of the LbL films. The decrease of charge density on polymer chains with varying pH, causes the chains to enter a coiled conformation state. Hence, the multilayers become swollen. Moreover, the coiled conformation increase might be associated with surface roughness increment. Consequently, upcoming polymer layer interacts better due to the increased roughness that resulted in increased surface area [62]. According to Rubner and co-workers, altering the pH of the solution causechanges in the development mechanism, composition, surface wettability, and thickness of multilayer films made of weak polyelectrolytes, i.e., polyacrylic acid (PAA) and poly(allylamine hydrochloride) (PAH) [63]. Li et al, studied the effect of pH of ALG solution (pH 3.0, 4.0 and 5.0) when depositing LbL films with CHI at pH 3.0. They observed that the thickness of films decreased with increasing pH of ALG solution. It was because the charge density of ALG increased with increasing pH, whereas the charge density of CHI remained same since pH of CHI solution was kept constant [64]. In another study of Rubner and co-workers, they investigated LbL self-assembly of CHI at pH 3.0 and 5.0 with polystyrene sulfonate (PSS) or carboxymethyl cellulose (CMC). They produced slightly thicker CHI/PSS multilayer films with CHI at pH 5.0 than that at pH 3.0 and attributed such result to CHI having lower charge density due to higher pH at 5.0. Thicker films are produced because of a decrease in the number of positive charges on the surface that coexist with a constant quantity of negative charges provided by the PSS layers. On the other hand, the CHI/CMC films produced by using CHI at pH 3.0 is significantly thicker than that of CHI at pH 5.0. Since CMC is a weak polyelectrolyte, the pH has a significant

impact on the development of the film. Most of the carboxyl groups in the CMC chains will be protonated at pH 3.0, and this will cause the polymer to stay in a coiled conformation, which will result in the development of thicker films. At higher pH levels, these groups will, however, become ionized, giving CMC chains an overall negative charge. This will increase electrostatic repulsion and cause the chains to adopt an extended conformation, which will result in thinner films. Since the electrostatic interactions between CMC and the CHI chains are considerably diminished at pH 3.0, thicker films were generated in the system. Also, it was important to pay attention to the difference in pH-dependent film growth trend between CHI/CMC and CHI/PSS. The film growth of multilayers constructed using CMC was affected by the deposition pH more than multilayers containing PSS. This was explained *via* non-electrostatic interactions (mainly hydrogen bonding) when CHI interacts with another natural polyelectrolyte which contributed to the film growth. Additionally, because the carboxyl groups in CMC are weak electrolytes, they are more susceptible to ionization than the sulfonate groups found in PSS. As a result, whereas the charge density of PSS chains is unaffected by pH in the investigated range, the CMC chains' charge densities and conformations changed depending on pH. However, because of being a weak polyacid, the charge density will vary depending on the medium pH for CMC [65].

1.4.3.2 Effect of Temperature

The temperature is another well researched component that has a significant influence on the stability, internal structure, morphology, thickness, and growth trend of multilayer assemblies. Several authors have reported on the impact of temperature on the polyelectrolyte multilayers' thickness. For instance, Van Patten and colleagues investigated how polyelectrolyte multilayer films made of PDADMAC and PSS changed with temperature and found that assemblies made at high temperatures were thicker than those made at room temperature because high temperatures caused the films to swell and allowed for greater interpenetration

between the polyelectrolyte layers due to loss of ionic interactions with increasing temperature [66]. Xu and co-workers studied temperature effect on hydrogen bonded multilayer films of poly(vinylpyrrolidone) (PVPON) and poly(acrylic acid) (PAA) at different temperature values between 10 °C and 60 °C and observed smoother film surfaces at high temperatures. The system they were working with showed different opacity at different film deposition temperatures. The films they produced below 20 °C were cloudy and opaque. However, the films were transparent if the film deposition was performed at temperatures above 25 °C. They tuned the opacity of their film by changing the deposition temperature, since the cloudier film resulted from the rougher surface which scattered more light. They also showed that bilayer of multilayers deposited at 50 °C was six-folds higher than the films constructed at 10 °C. They suggested that their film growth showed different characteristics in the cloudy region (below 20 °C) compared to that in the transparent region (above 25 °C). In the cloudy area, the increase in film thickness was associated with conformational change of polymers. PVPON and PAA performed poorly at blending and the surface was rough in the cloudy region, whereas they performed well at blending and the surface was smooth in the transparent region [67]. Volodkin and co-workers also studied the effect of temperature on film growth composed of poly(L-lysine)/hyaluronic acid (PLL/HA) multilayers constructed within a temperature range of 25–85 °C through LbL deposition. They obtained thicker and more porous/permeable film structures at higher temperatures. They explained this phenomenon by polymer diffusion, conformation, and inter-polymer interactions:

i. Polymer Diffusion

Volodkin and co-workers suggested that free PLL molecules quickly diffused into the film during PLL deposition, and then diffused out, complexed with HA at the top of the film during HA deposition. This complexation caused increase in film thickness. As a result, the growth rate was strongly influenced by the diffusive movement of PLL. The diffusion constant strongly depends on temperature due to its nature;

$$D = D_0 e^{-E_{aD}/RT}$$

where;

D: diffusion coefficient,

D_0: frequency factor,

E_{aD}: activation energy for diffusion,

R: gas constant,

T: temperature in Kelvin

Therefore, increase in temperature resulted in increased mobility of free polymer chains, causing more polymer diffusing into the multilayer structure during build-up process, finally increased rate of film growth [68].

ii. Polymer Conformation

Volodkin and co-workers suggested that the new polymer would penetrate the coating more noticeably at higher temperatures. According to the findings of their neutron reflectivity studies, conformations of the polyelectrolytes changed from extended to coiled form. Due to intramolecular alterations, or reduced attraction between charges in the polymer backbone at higher temperatures, this structural change occurred. In summary, as the film deposition temperature changes, the conformation of the polymers also change, resulting in diversity in film characteristics.

iii. Inter-polymer Interactions

Volodkin and co-workers suggested that there were two distinct aspects in which the inter-polymer interactions caused by ion pairing affected the rate of film growth. The inter-polymer association became weaker as the temperature rose, increasing the polymer mobility in the multilayers and encouraging the dissociation of ionic interactions. This would speed up the development of the film as mentioned above and boost the polymer diffusion into the film. However, annealing might also cause the films to become less permeable as the temperature rose. A maximum number of

ion pairs was suggested to be achieved by polymer chains for the specified stoichiometric interaction due to the improved polymer mobility. On the other hand, annealing the polymer network lessened the network's defects and made it denser and more impermeable to diffusion of polymers [68].

1.4.3.3 Effect of Salt Concentration

For examining the stability, permeability, internal structure, function, and development of multilayer systems constructed by electrostatic interactions and hydrogen bonding; salt concentration has also been one of the extensively examined factors. In this regard, Dubas and Schlenoff described the development of PEM films made up of PDADMAC (poly(diallyl dimethyl ammonium bromide)) and PAA or PSS as well as how the salt concentration affected the thickness of multilayers. Film thickness rose up to a salt concentration of 0.3 M before rapidly decreasing and completely dissociating at a salt concentration of 0.6 M or higher. It was suggested that the film dissociated due to competition between the salt ions and polyelectrolyte pairs [69].

The effect of salt content on the structure of polyelectrolyte multilayers (PEM) was also studied by Caruso et al. They showed how salt-induced structural changes resulted in nanoporous PEMs, demonstrating how ionic strength could be employed to regulate the permeability of multilayer films. The scientists also examined how salt affected the morphology and mechanical characteristics of hollow capsules made of PSS/PAH layers. They discovered that high salinity levels (>3 M) caused the membrane of PSS/PAH capsules to soften noticeably, which caused the capsules to shrink [70].

1.5 Layer-by-layer Applications of Chitosan and Alginate

CHI and ALG are frequently preferred as LbL assembly components for various applications. For example, Gao and co-workers deposited CHI-ALG multilayers on

titanium surfaces and encapsulated minocycline (as antibacterial agent). In this study, possible application was coating of titanium implants for dentistry applications [71]. In another research conducted by Zhou et. al., antifouling properties of CHI-ALG multilayers were examined. Their findings obtained from QCM-D showed that albumin (protein) could not be deposited onto multilayer coated film surface. The results were similar regardless of the topmost layer, i.e., CHI or ALG. Moreover, they suggested that CHI/ALG multilayer coatings can be a strong alternative to PEGylated surfaces in case of preventing protein adsorption [72]. Zheng and co-workers applied the multilayer coating on doxorubicin loaded nanoparticles and studied drug release properties for tumour treatment applications. They observed improved drug release regime, and the undesirable burst release was decreased from 55.12% to 5.78%. Moreover, they reported that coated nanoparticles showed anti-tumour efficiency with 83.17% tumour inhibition rate. Finally, they suggested that the multilayer coating decreased the toxicity in comparison with non-coated nanoparticles [73]. Finally, Kim et. al. used CHI/ALG multilayer coating on shrimp as antimicrobial edible coating. They incorporated grapefruit seed extract as antibacterial agent into multilayers. They analysed bacteria amount for 15 days at 4°C. After 14 days, they observed 2 log orders of decrease in bacterial count [74].

1.6 Incorporation of Bacteriophages in Antibacterial Surface Coatings

The number of studies in this area are very limited. Lin and co-workers encapsulated bacteriophages in liposomes. They formed a surface coating by blending the phage-encapsulated liposomes with CHI solution. The thickness of the film they produced for the study was 9 cm. They examined the antibacterial efficiency of their film against *E. coli* O157:H7 in beef. After 15 days, they observed 4.55 log CFU/g of decrease in bacterial count [75]. Müller and co-workers adsorbed bacteriophages onto 5-layers of branched poly(ethyleneimine) and poly(acrylic acid) coated surfaces and observed antibacterial activity against *E. coli* and *S. aureus*. They designed the coatings to be used in implant applications. They observed improved adsorption of

phages with the multilayers having positively charged topmost layer. The reason for this was associated with better electrostatic interactions between multilayer films and the anionic capsid proteins of bacteriophages [76]. Finally, Francius and co-workers studied infectivity of bacteriophages when they were incorporated to multilayer films. They worked with several polyelectrolyte pairs, for example poly(L-lysine) and hyaluronic acid or poly(allylamine hydrochloride) and poly(acrylic acid). They compared the performance of the bacteriophage loaded multilayers and offered a comprehensive study for the effect of charge of the multilayer components on infectivity on bacteriophages [77].

1.7 The Aim of the Thesis

The overall aim of this thesis study was to prepare an ultrathin polymer platform capable of encapsulating and releasing bacteriophages for food packaging applications. In this context, the following objectives were aimed to be accomplished:

1. To find a suitable biopolymer pair for successful deposition of ultrathin multilayer films through layer-by-layer technique.

2. To characterize these multilayers with respect to physicochemical properties such as growth profiles, stability, surface morphology.

3. To characterize bacteriophages and design the proper multilayer structure for efficient loading of bacteriophages.

4. To examine the antibacterial activity of bacteriophage loaded multilayer films.

5. To contrast the antibacterial activity of bacteriophage loaded multilayer films with antibacterial activity of multilayers containing commonly used antibacterial molecules which are safely considered to be used in food technology applications.

CHAPTER 2

EXPERIMENTAL

2.1 Materials

Sodium Alginate (NaALG) (viscosity of 15–25 cP, 1% in H_2O) (mannuronate/guluronate (M/G) ratio=1.56) (M_w 120000-190000 Da), Low molecular weight Chitosan (M_w 50000–190000 Da and % 75–85 deacetylated) (CHI) obtained from Sigma Chemical Co., Luria-Bertani (LB) (1.5%) agar, Acetic acid (≥ 99 %), Curcumin (CUR) from Curcuma longa (>65%), Ciprofloxacin (CIP) (≥ 98 %, HPLC), Lactic acid (LA) (Merck Chemicals, 90%), Thymol (THY) (Merck Chemicals, M_w=150.22 g/mol), Sulfuric acid (H_2SO_4) (98%), Sodium chloride (NaCl) purchased from Carlo Erba, Sodium hydroxide (NaOH) (Pellets), Sodium dihydrogen phosphate dihydrate ($NaH_2PO_4.2H_2O$), TA (M_w=1701.20 g/mol) were purchased from Merck Chemicals. The deionized (DI) water was purified by passage through a Milli-Q system (Millipore) at 18.2 MΩ.

2.2 Deposition of CHI-ALG multilayer films on Silicon Wafers/Glass Slides

For cleaning purposes, silicon wafers and glass slides (1 cm x 1 cm) were immersed in concentrated sulfuric acid solution for 85 minutes, rinsed with deionized water and dried under continuous nitrogen gas flow. Then, the substrates were soaked in 0.25 M NaOH solution for 10 minutes, rinsed with water and dried under nitrogen gas flow.

0.5 mg/mL chitosan was dissolved in 0.1% (v/v) acetic acid solution at 25 °C overnight. pH of the polymer solution was fixed at 5.0 prior to use. 0.5 mg/mL

alginate solution was prepared in DI water at 25 °C one night prior to use. Solution pH was adjusted to 3.0 before LbL process. Either silicon wafers or glass slides were dipped into the chitosan solution for 10 minutes. Substrates were rinsed 2 times with 0.1% (v/v) acetic acid solution at pH 5.0 for 2 minutes each. The same process was repeated for alginate layer deposition. pH of the water was adjusted to 3.0 with pH-meter and used for rinsing of ALG layers. This polymer deposition cycle was repeated until desired number of polymer layers were deposited at the substrate surface.

2.3 Stability Studies of (CHI-ALG) Multilayer Films

CHI/ALG LbL films were immersed separately into 0.9% (w/v) NaCl solution at pH 7.0, 20% (v/v) EtOH-Phosphate buffer (10^{-2} M, pH 5.0), and phosphate buffer at pH 5.0 and 7.0 in a Lauda Alpha RA 8 chiller circulator with the temperature adjusted to 25 °C for 18 hours. Film thickness was measured before and after immersion into the solutions mentioned above and the fraction retained at the surface was calculated by dividing the film thickness after treatment to the initial film thickness.

2.4 Preparation of Phage and Bacteria Solutions

In this study, *Salmonella enterica* subsp. *enterica* serovar Enteritidis (MET S1-001) was used as the model pathogen due to its prevalence in foods. The strain was isolated from food (chicken meat) during the previous studies of Soyer Lab. The bacteriophages do not include antimicrobial resistance and virulence genes and considered as GRAS (generally recognized as safe) [78,79]. Isolate was stored at -80 °C, at METU Food Safety laboratory and cultured on brain heart infusion (BHI) media prior to experiments.

Phage (MET_P1_001_43) was isolated from cattle manure by using (MET S1-001) as target host at Soyer Lab. The phage is a lytic phage with 43205 bp genome. Genome sequence is available on NCBI (accession number: OP389270). Fresh

phage solutions were prepared before experiments and adjusted to 10^8 plaque forming units per millilitres (PFU/mL) by using 0.9% NaCl solution and confirmed by double plaque assay (DPA) [78].

2.5 Bacteriophage Enumeration

In every experiment, DPA was performed to determine the phage counts in film loading solutions and loaded films. Luria-Bertani (LB) (1.5%) agar was used as base agar. 100 µL host bacterium (S1-001) and 100 µL phage loading solution was added into LB top agar (0.6%), gently swirled, and poured onto base agar. Plates were kept on the bench for ten minutes to let top agar solidify and incubated 37 °C for 18-20 hours [78].

2.6 Bacteriophage Loading to CHI-ALG Multilayers

CHI-ALG films with varying number of layers were prepared on glass slides as described in section 2.2. Multilayer films were then immersed into 10^8 PFU/mL phage solution containing 0.9% (w/v) NaCl in a Lauda Alpha RA 8 chiller circulator at 25 °C for 18 hours. During the phage encapsulation process, 10 mL of phage solution was used for each multilayer film (1 x 1 cm^2). Three replicates for each 1-layer CHI, 11-, 41- and 71-layers CHI/ALG phage loaded films were prepared for every Disc-diffusion test. pH of phage solution was maintained at 7.0 prior to use.

2.7 Loading of Antibacterial Molecules: CUR, THY, LA, TA & Antibiotic: CIP into CHI-ALG Multilayer Films

$(CHI\text{-}ALG)_{20}$-CHI multilayer films were prepared as described in section 2.2. Curcumin (CUR), thymol (THY), lactic acid (LA), and tannic acid (TA) were chosen as antibacterial reagents. 0.2 mg/mL CUR was dissolved in 20:80 (v/v) Ethanol (EtOH):Phosphate buffer (10^{-2} M) and pH of the solution was adjusted 5.0. 1 mg/mL

THY was dissolved in 20:80 (v/v) Ethanol (EtOH):Phosphate buffer (10^{-2} M) and pH of the solution was adjusted 7.0. 1 mg/mL LA and TA solutions were prepared in 10^{-2} M phosphate buffer and pH was adjusted to 7.0 before encapsulation process. For each system three film replicates were prepared and for each multilayer film 10 mL of antibacterial molecule solution was used.

CHI/ALG multilayer films were deposited onto glass slides as described in section 2.2. They were immersed into 0.1 mg/mL ciprofloxacin solution at pH 7.0 (prepared in 10^{-2} M phosphate buffer) and 25 °C for 18 hours. 10 mL of ciprofloxacin solution was used for each substrate. CIP encapsulated films were used as positive control for each CHI/ALG multilayer film for disc-diffusion tests.

All encapsulation processes were carried out in a Lauda Alpha RA 8 chiller circulator with the temperature adjusted to 25 °C for 18 hours.

2.8 Disk-Diffusion Test

Effectiveness of phage loaded films on Salmonella Enteritidis was determined by Kirby Bauer test as described by Hudzicki [80]. Mueller Hinton (MH) agar plates were prepared before the analysis and waited and labelled at room temperature prior to experiments. Inoculum was prepared in the log phase in MH broth. Concentration of inoculum was adjusted with a sterile saline (0.9%) solution to 0.5 McFarland standard by using a densitometer (DEN-1B) and used in 15 minutes. Bacteria inoculated onto MH agar by streaking a sterile swab three times.

Agar plates containing MH broth were prepared according to the manufacturer's instructions and pH was adjusted to 7.0 or 5.0. A volume of 100 µL of *Salmonella enterica* serovar Enteritidis was spread-plated on MH agar separately. For each system 5 different films of CHI/ALG were prepared. One of them was used as blank and one of them was loaded with CIP and used as positive control. Three of each set of films were used for the antibacterial activity tests, calculation of average zone

sizes with the standard deviations provided by phages or any other antibacterial molecule under investigation.

Phage loaded multilayer films were placed onto the middle of the agar plate. The plates were incubated at 37 °C for 20 hours. The zones were visualised with GelDoc Go image system (Bio-Rad, USA). In every experiment, three independent films were placed as well as a blank control and a ciprofloxacin loaded film as the positive control.

2.9 Instrumentation

Hydrodynamic size and zeta potential measurements of bacteriophages were performed using Zetasizer Nano-ZS (Malvern Instruments Ltd., U.K.). The concentration of bacteriophages in 0.9% NaCl solution at pH 7.0 and 5.0 was ca. 10^8 PFU/mL. Zeta potential value is estimated with the help of electrophoretic mobility *via* Smoluchowski approximation. Hydrodynamic size measurements of bacteriophages were carried out *via* DLS technique using a cumulants analysis based on the autocorrelation data.

Ellipsometric thickness of LbL deposited multilayer films on silicon wafers were measured using a Optosense, USA (OPT-S6000) ellipsometer.

QCM-D sensor was obtained from Biolin Scientific, QSense Sensors, QSX 301. Sensor surface was quartz crystal coated with gold (Au). For preparation of the experiments performed with the QCM-D, the sensor (QSX 301) was pre-equilibrated with rinsing solution of CHI (0.1% acetic acid solution at pH= 5.0) for a minimum of 30 min to establish a stable baseline. Multilayer deposition on the surface is performed with 0.5 mg/mL CHI (in 0.1% acetic acid, at pH 5.0) and ALG (in DI, at pH 3.0) polymer solutions, for 10 minutes. Rinsing is performed with 0.1% acetic acid (pH 5.0) after CHI and DI (pH=3.0) after ALG deposition for 10 minutes. Polymer and rinsing solutions purged into the sensor chamber with a flow rate of

150 μL/min. After each layer deposition, change in frequency (Δf) data gathered and mass change is estimated using Sauerbrey equation [81].

Atomic force microscope (AFM) imaging of the films was performed using a NT-MDT Solver P47 AFM in tapping mode with Si cantilevers. Multilayer films were deposited onto 1.0 cm x 1.0 cm glass slides for AFM imaging studies.

Transmission electron microscopy (TEM) images of phages were obtained using a FEI Tecnai G2 Spirit Bio-Twin CTEM instrument operating at an acceleration voltage of 20–120 kV. Phages were stained with phosphotungstate solution (2.0% (v/v), pH 7.2) before imaging.

CHAPTER 3

RESULTS AND DISCUSSION

3.1 LbL Assembly and Surface Morphology of CHI/ALG Multilayer Films

CHI and ALG were self-assembled at the surface of silicon wafer, glass slide or gold-quartz crystal sensor through LbL technique. CHI has pK_a value around 6.5 [82]. pK_a values of guluronic acid and mannuronic acids of ALG are around 3.4 and 3.6, respectively [22]. Deposition of CHI and ALG was performed at pH 5.0 and 3.0, respectively. The deposition pH of ALG was close to its pK_a. Therefore, ALG was partially ionized at pH 3.0. On the other hand, CHI was deposited below its pK_a. Therefore, the primary amino groups of CHI were mostly in the protonated form. Scheme 5 shows chemical structures of CHI and ALG and their pK_a values. The primary driving force for LbL growth was electrostatic interactions between protonated amino groups of CHI and carboxylate groups of ALG. In addition, hydrogen bonding interactions between hydroxyl and amino groups of CHI and protonated carboxylic acid and hydroxyl groups of ALG might have contributed to polymer complexation at the surface [83].

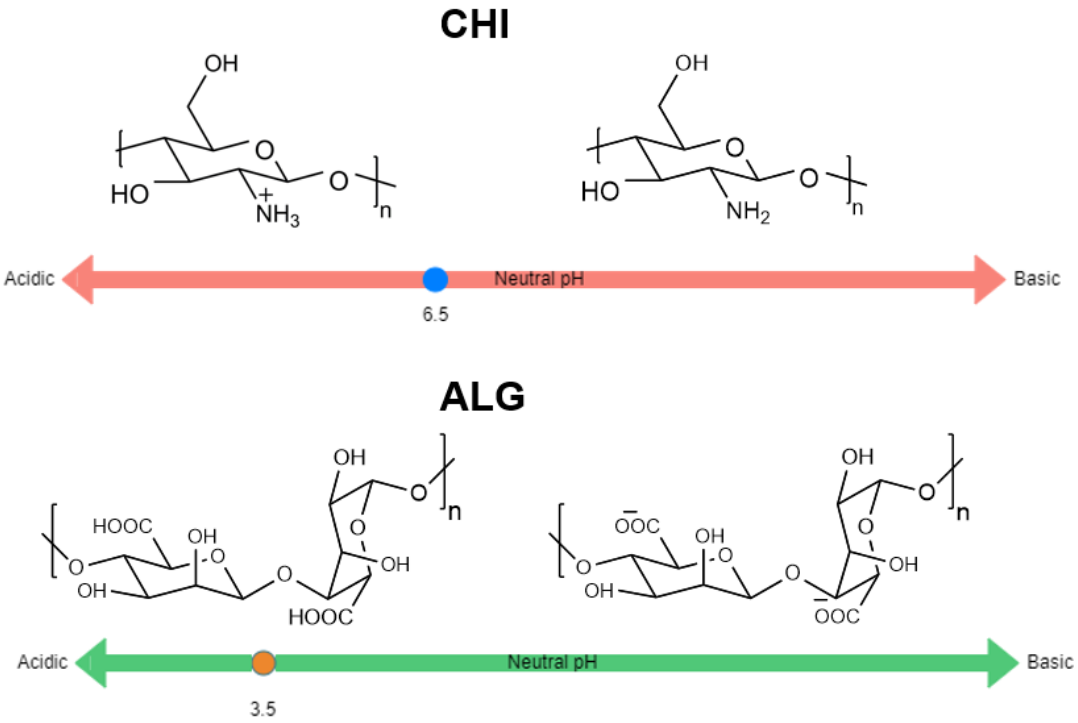

Scheme 5. p*Ka* dependent chemical structures of CHI and ALG.

LbL growth of CHI/ALG multilayer films was followed using ellipsometry and quartz crystal microbalance with dissipation (QCM-D) techniques. Ellipsometry analyses the polarization change that occurs when light reflects off or passes through a material. The phase difference in signal and change in amplitude ratio of polarized light on different planes are used to indicate the polarization-change. The optical characteristics and thickness of the material have an impact on the observed response. As a result, ellipsometry is mostly employed to calculate optical constants and film thickness [84]. Ellipsometric thickness measurements of CHI/ALG LbL films showed linear growth profile with a linear regression (r^2) score of 0.99884 (Fig. 1). The increase in film thickness per layer was ~3 nm.

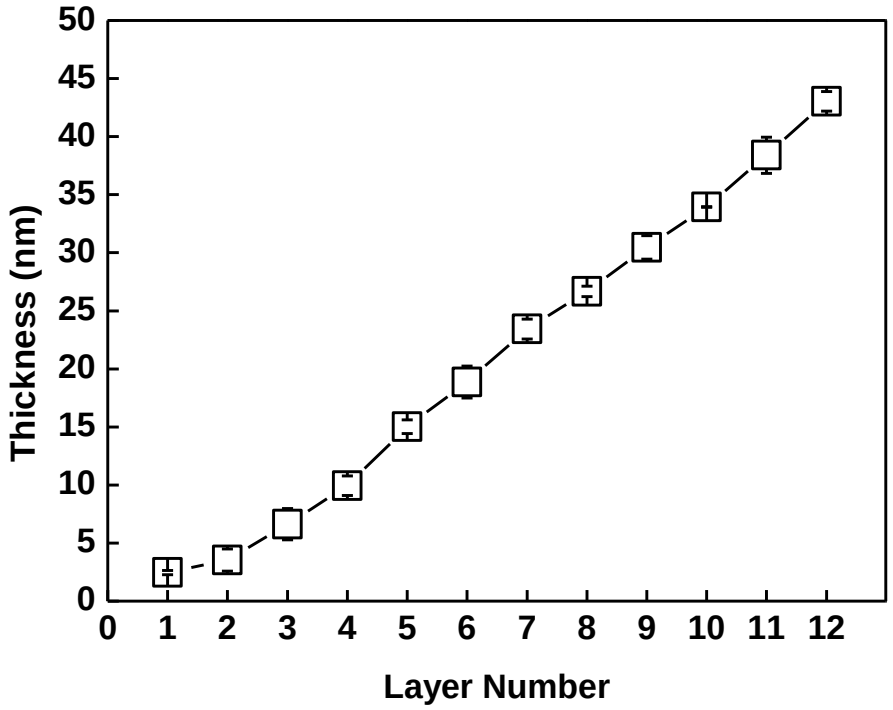

Figure 1. LbL growth of CHI and ALG; Ellipsometric thickness values are plotted as a function of layer number.

QCM-D is widely used to follow entities such as polymers, proteins, organic molecules, nanoparticles, ceramic matrices etc. accumulating on surfaces. The principle behind the process depends on an "on and off" voltage applied periodically, hence vibrating the quartz at its resonance frequency. Any additional mass on the sensor causes the resonant frequency to decrease. The Sauerbrey equation (Equation 1) is used to relate the mass intake (Δm) to the frequency change (Δf) for thin films;

Equation 1. The Sauerbrey equation.

$$\Delta m = -C \times {}^{\Delta f}/_{n}$$

In Sauerbrey equation, C ($ng/(cm^2 \times Hz)$) is mass sensitivity constant and related to the specifications of quartz, n is the overtone number, which is related to the number of the harmonic, and Δf (Hz) is the frequency at a given time, obtained from

the spectrum [81]. Unlike the linear LbL growth profile determined through ellipsometry, QCM-D measurements showed exponential growth pattern for CHI/ALG multilayers (Fig. 2).

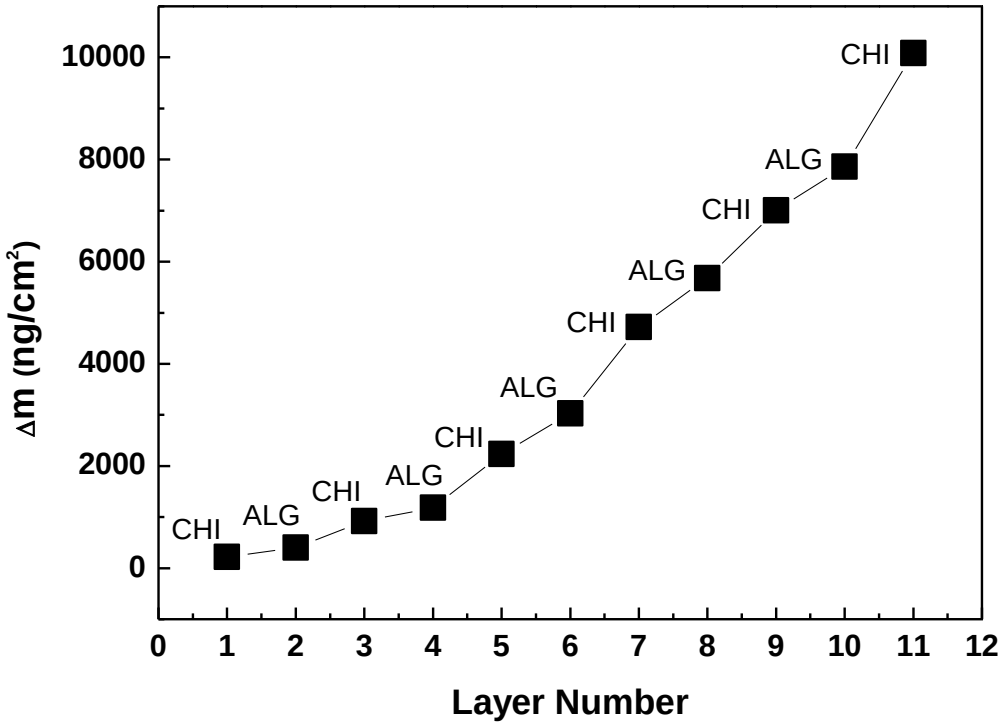

Figure 2. Mass increment with respect to layer number for LbL deposition of CHI and ALG obtained from QCM-D.

The difference in the film growth profiles determined through ellipsometry and QCM-D was attributed to the sample preparation and measurement conditions. For ellipsometric film thickness measurements, the substrate was first dipped into CHI solution for 10 minutes, followed by the rinsing step to remove the loosely bound polymers. Then, the substrate was dried under nitrogen gas flow prior to film thickness measurement. Similar steps were followed for deposition of ALG layers. On the other hand, QCM-D measurements were performed in-situ. In other words, CHI or ALG solution was purged into the chamber containing the substrate and the

change in frequency was measured simultaneously. When the polymer deposition was finalized (indicated by reading the frequency signal at a fixed value), the rinsing step was performed. Rinsing step led to a slight increase in frequency due to removal of the loosely bound polymer chains from the surface. When the signal was levelled off, ALG solution was purged into the chamber. Of note, there are no drying steps between purging of the polymer solutions to the chamber and deposition of layers. To further confirm the effect of drying process between the layer depositions on the LbL growth profile, 3-, 6-, 9- and 12- layers of CHI and ALG were deposited separately onto 4 different substrates and the drying process was performed not after each layer deposition but at the end of film preparation. Thickness measurements were performed through ellipsometry, and the thickness values were contrasted with the films in which drying was performed after each layer deposition. Figure 3 contrasts the thickness of the films with the same layer number prepared with and without drying process after each layer deposition. Ellipsometric thickness measurements of non-dried films demonstrated exponential-like film growth with an exponential regression value of 0.9917 which was closer to the ideal value (1.0) than linear regression value of 0.9768. This result was in good agreement with the exponential growth profile determined through QCM-D, confirming the effect of drying process on film thickness and growth trend.

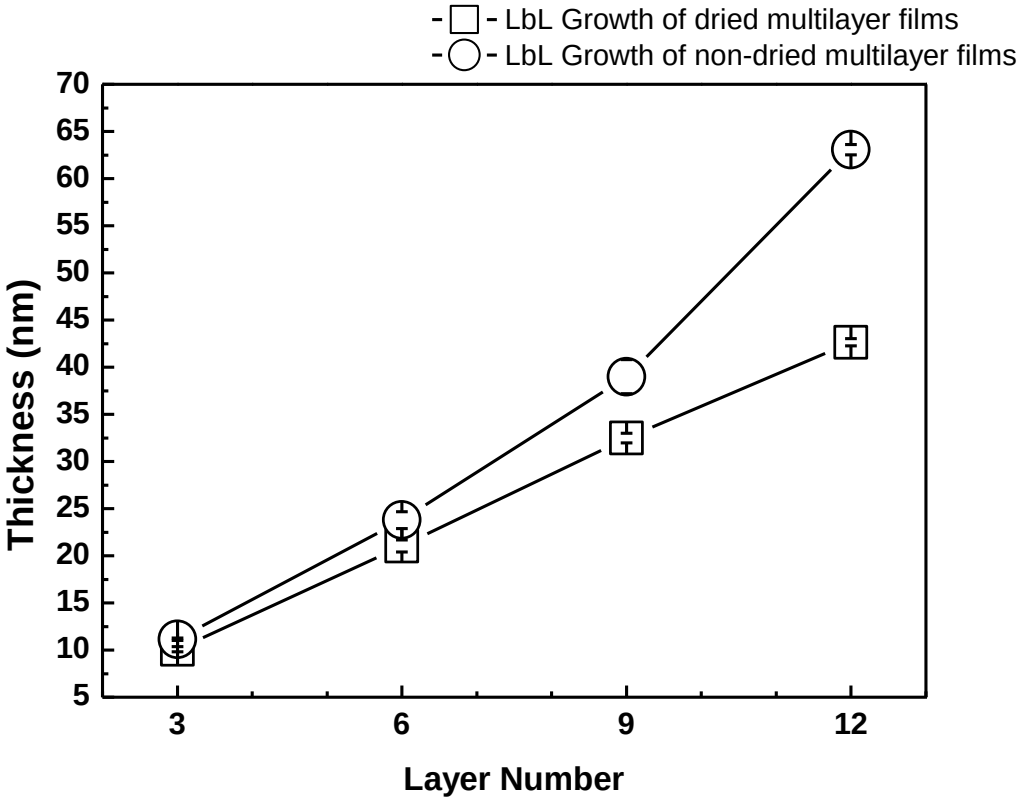

Figure 3. Ellipsometric thickness of CHI/ALG multilayer films as a function of layer number. Data that belong to multilayer deposition with drying after each layer deposition is shown with squares. Data that belong to multilayer deposition without drying steps is shown with circles.

Exponential growth in LbL self-assembled films is observed when the surface roughness increases with increasing layer number. This is because the increasing surface roughness provides additional surface area for deposition of the polymers at the surface. Alternatively, exponential growth is observed due to "in and out" diffusion of at least one of the polymers during LbL process. These weakly bonded chains diffuse from the inner layers to film-solution interface, and complexes with the depositing polymer. These complexes cause higher mass deposition on the substrate, thicker, rougher, and more porous film structure [68]. This effect becomes more remarkable as the layer number in the film increases.

It must be borne in mind that both CHI and ALG were deposited at pH close to their pK_a values. Therefore, both were partially ionized at the deposition pH. The relatively weak association (low binding points) between CHI and ALG (compared to fully ionized states) might have resulted in more loopy conformation of the polymer chains and increased surface roughness [58,85]. To investigate the change in surface roughness with respect to layer number, AFM analysis was performed to 11-, 41- and 71-layer CHI/ALG films (Fig. 4). Surface roughness analysis through AFM showed that roughness of CHI/ALG multilayers increases significantly as more layers are deposited at the surface. For instance, average roughness for 11-, 41- and 71-layer films were 69.0 nm, 336 nm, and 599 nm, respectively. Therefore, the exponential growth of CHI/ALG films was attributed to the increased surface roughness, providing additional area for polymer deposition.

The difference in the growth profiles of dried and non-dried films was attributed to the drying process under N_2 flow which might have induced rearrangement of the polymer chains at the surface. The drying might have induced ordering of the polymer chains and reduced the interpenetration among the layers. This might have led to formation of more stratified layers with relatively low number of loops and tails within the film, thus relatively low surface roughness. For this reason, exponential growth regime was not observed with the films in which surfaces were dried under N_2 flow after each layer deposition.

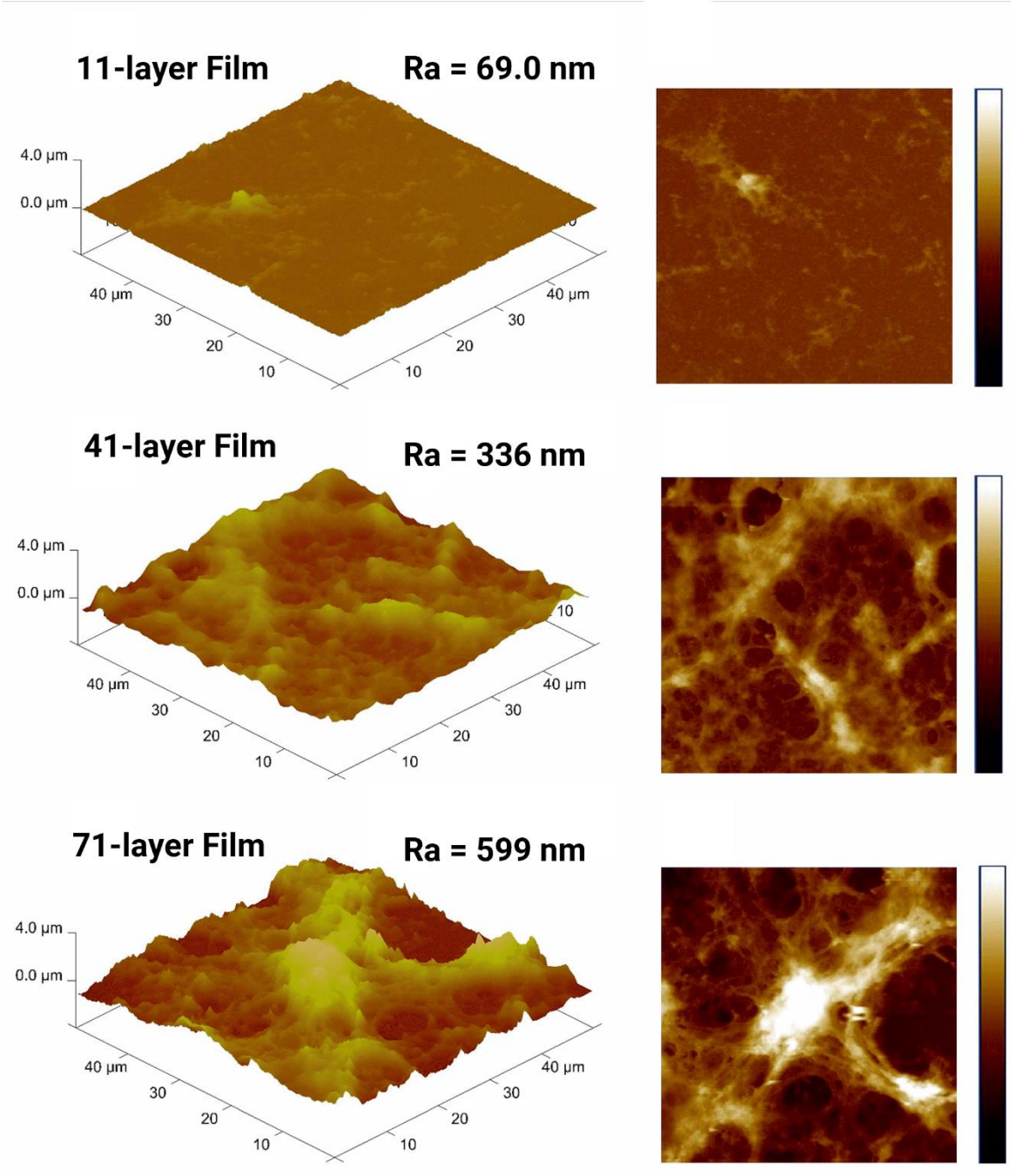

Figure 4. AFM roughness values (Ra), height (left) and topography (right) images (50 × 50 µm scan size, hmax = 4.0 µm) of (CHI-ALG)n-CHI films with layer numbers; 11-layer, 41-layer, 71-layer.

Non-dried films were used for the rest of the study due to practical reasons. For bacteriophage loading studies, 11-, 41- and 71-layer films were of interest to see the effect of layer number on the bacteriophage loading. However, the thickness of the films with relatively high layer numbers could not be measured through ellipsometry because the light was strongly absorbed by the film surfaces. Thus, incident beam could not be reflected from the surface and the intensity of the beam reached to the detector was not enough to make reliable measurements. For this reason, vertical distance analysis was performed using AFM to measure the film thicknesses. The vertical distance of 11-layer, 41-layer and 71-layer film was found as 48.3 ± 8.4 nm, 697 ± 112 nm, and 2043 ± 412 nm, respectively (Fig. 5). These thickness values were in good agreement with the exponential growth profile observed using ellipsometry and QCM-D techniques for multilayers prepared without a drying step after each layer deposition.

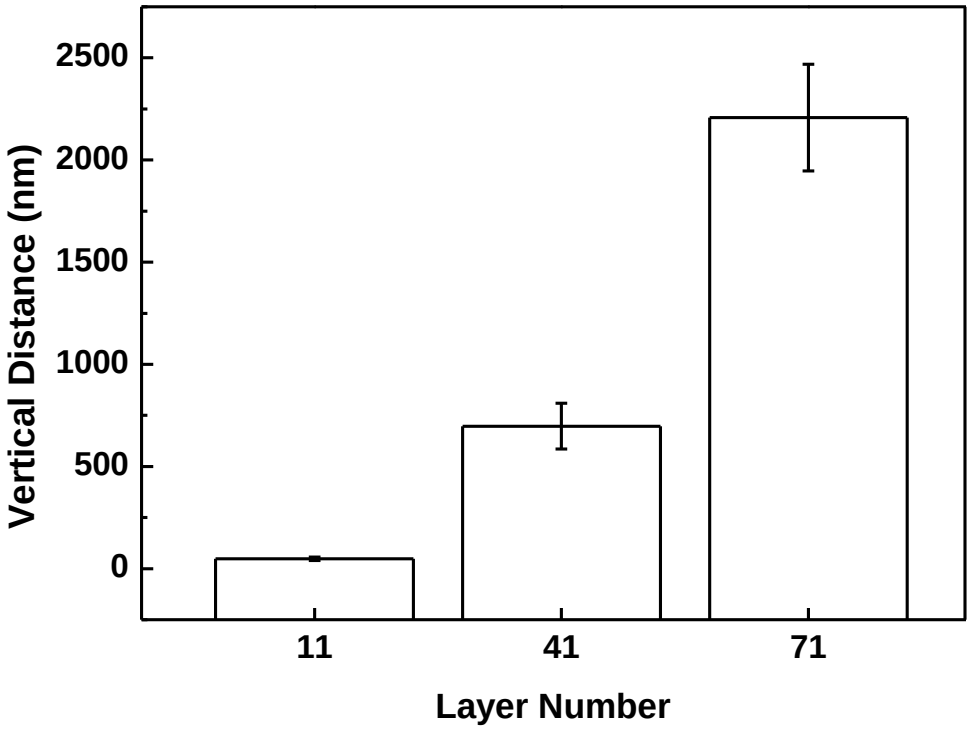

Figure 5. Vertical distance analysis of 11-, 41- and 71-layer films through AFM imaging.

3.2 Characterization of Bacteriophages

Bacteriophages were characterized through hydrodynamic size measurements through DLS technique, zeta potential measurements and TEM imaging. Figure 6 shows the hydrodynamic size distribution curve by intensity and number. The distribution by intensity showed a single peak with a maximum at ~200 nm, whereas the distribution by number plot showed a single peak (average size ~160 nm) with a tail in the larger size of the distribution, possibly arising from the presence of few aggregates. The zeta potential of bacteriophages (dispersed in normal saline solution) was measured as -8.8±1.1 mV at pH 7.0 and -7.8±1.1 mV at pH 5.0.

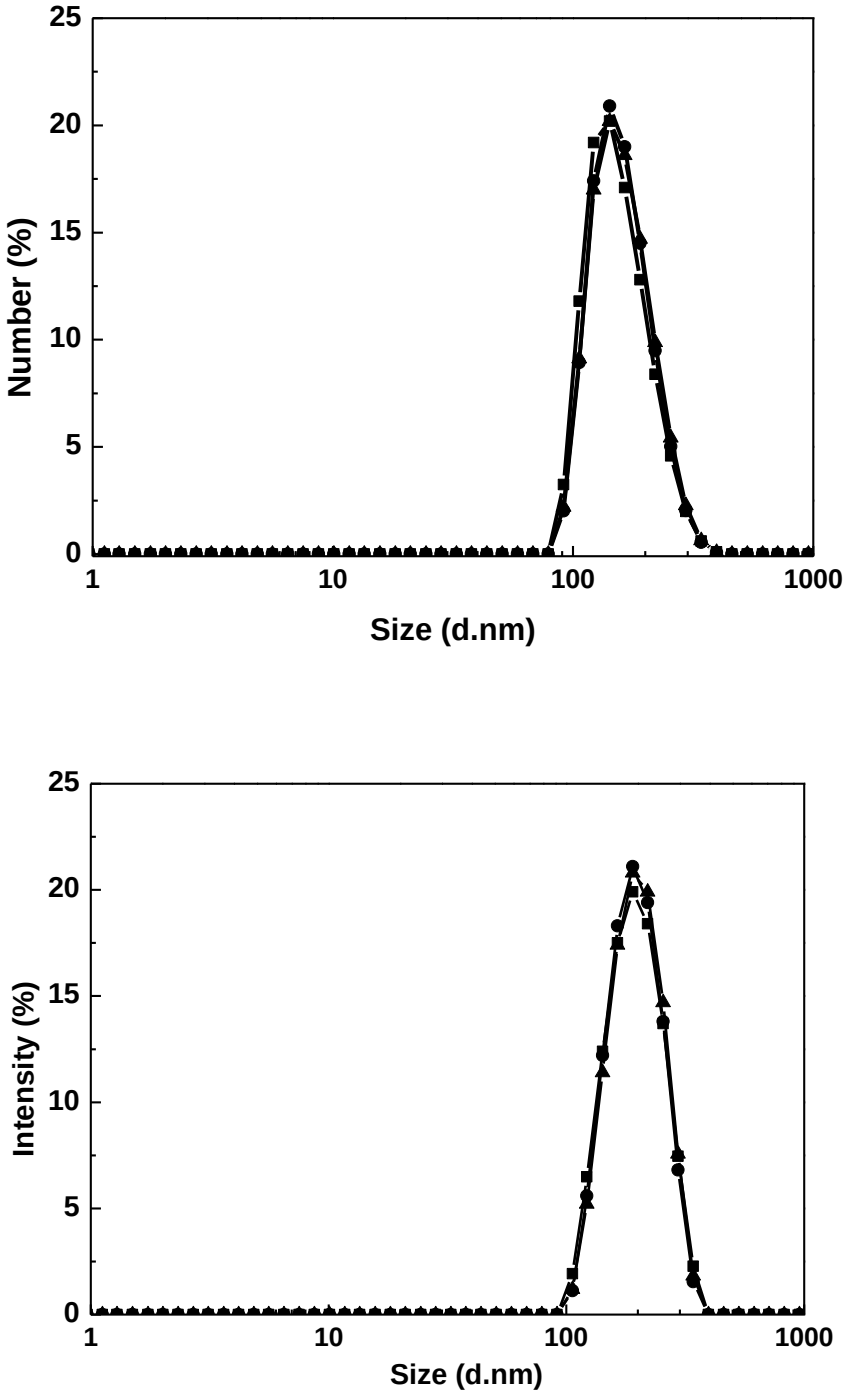

Figure 6. The hydrodynamic size distribution of bacteriophages by number and intensity.

TEM images clearly show the head and tail parts of the bacteriophages (Fig. 7). According to size measurements *via* TEM imaging, the head part of a phage was around 50 nm and the long tail was around two times longer than the head [78]. These values were in good agreement with the size obtained through DLS measurements.

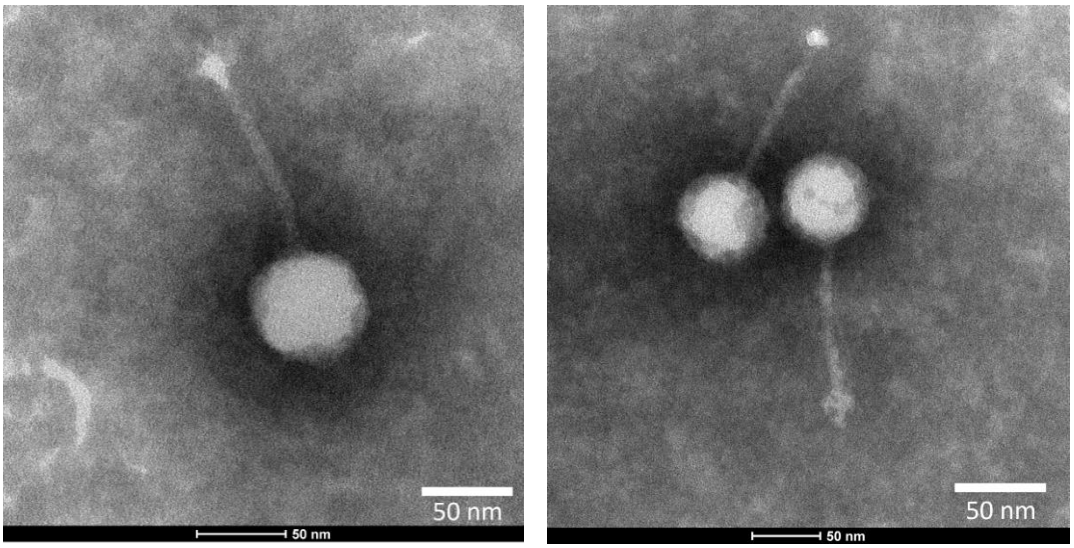

Figure 7. TEM images of bacteriophages.

3.3 Stability of (CHI-ALG) Multilayer Films

Prior to loading CHI/ALG LbL films with bacteriophages (Section 2.6), stability of the films was examined under conditions (pH 7.0, 18 hours at 25 ℃) at which loading of bacteriophages would be conducted. Bacteriophages were dispersed in a buffer solution containing % 0.9 NaCl. Therefore, 11-layer CHI/ALG film was immersed into normal saline solution (% 0.9 NaCl) at pH 7.0 and 25 ℃ for 18 hours. Of note, several antibacterial agents such as curcumin, thymol, tannic acid, and lactic acid were also loaded into CHI/ALG multilayers for comparison of the antibacterial activity to those of bacteriophages (Section 2.7). Among these antibacterial agents, curcumin and thymol were not soluble in buffer solution. Therefore, both were dissolved in a buffer containing 20% ethanol in volume (pH 7.0) in the loading

process. For this reason, stability of multilayers was also examined in a mixture of phosphate buffer and ethanol with 80:20 v/v ratio.

Besides the loading conditions, stability of multilayers was also assessed at acidic conditions prior to antibacterial activity studies. This is because pH ranges between slightly acidic and neutral pH values in carcass meat. For example, pH for carcass broiler chicken meat is around 5.7 [86].

The film thickness was followed as a function of time through ellipsometry. The fraction retained at the surface was calculated by dividing the thickness values by the initial thickness of the film and the decrease in the fraction retained at the surface was correlated with the loss of polymer layers (instability of the films) from the surface. It is worth to mention that although antibacterial activity studies were conducted with 11-, 41- and 71-layer films, stability of multilayers was examined with 11-layer CHI/ALG films. This is because the evolution of thickness was followed through ellipsometry and for CHI/ALG films, reliable thickness measurements could be obtained when the layer number exceeds 12, due to significant decrease in the intensity of light reflected to the detector of the instrument.

As seen in Figure 8, more than 90% of the films retained at the surface under all conditions mentioned above. The slight increase in thickness (fraction retained >1) was attributed to the water entrapped within the multilayers after exposure to aqueous solutions for 18 hours.

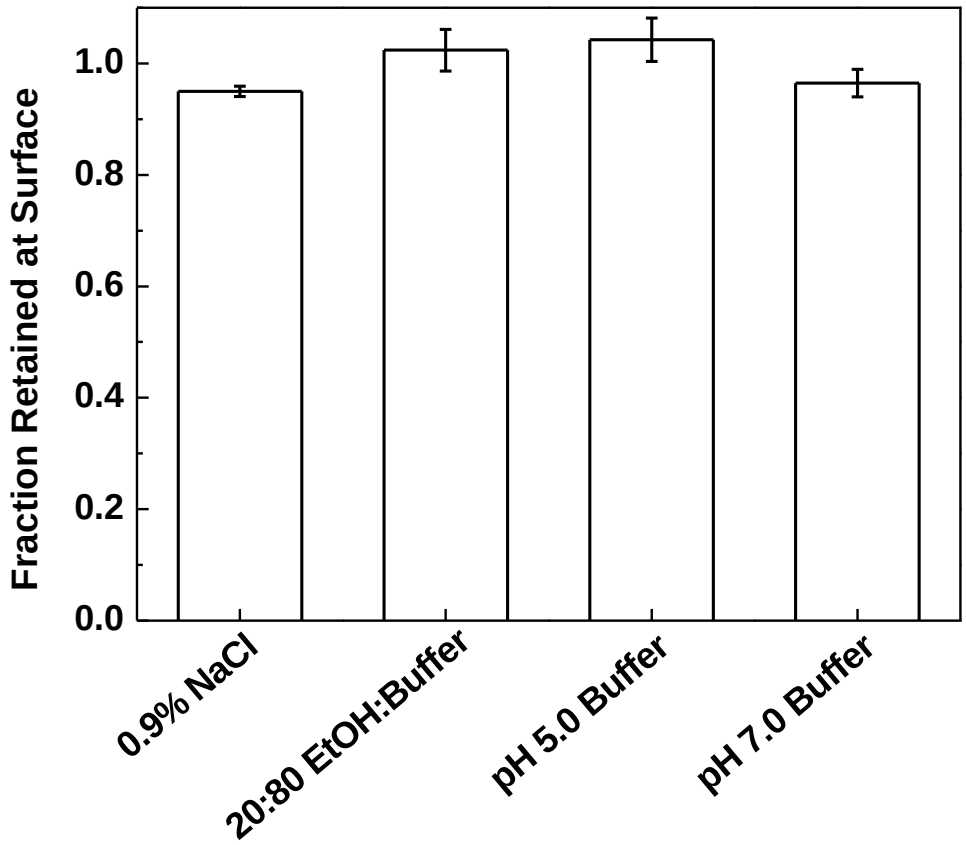

Figure 8. Fraction retained at the surface of 11-layer CHI-ALG films in 10 mM phosphate buffer containing 0.9% NaCl at pH 7.0, 80:20 (v/v) 10 mM phosphate buffer:ethanol at pH 7.0, 10 mM phosphate buffer at pH 7.0 and pH 5.0.

3.4 Bacteriophage loading to LbL Assembly of CHI-ALG Multilayer Films

Zeta potential measurements showed that bacteriophages carried negative charge. Therefore, the positively charged component of the multilayer film, CHI, was selected as the topmost layer for bacteriophage loading studies to obtain utmost interactions with the LbL coating and maximize bacteriophage loading. Of note, CHI has a pK_a of 6.5 [87] and is not fully ionized at pH 7.0. Still, the association of partially positively charged CHI and negatively charged bacteriophages was expected to be greater than that between negatively charged ALG and

bacteriophages. In addition to electrostatic interactions between phages and CHI, loading of phages could have also occurred through self-diffusion of phages into the multilayers due to weakening of the association among the layers at pH 7.0. It must be borne in mind that CHI and ALG films were deposited at pH 5.0 and the association among the layers weakened with increasing pH due to deprotonation of CHI.

3.4.1 QCM-D analysis

Bacteriophage loading to multilayers was followed through QCM-D. First 11-layers of CHI and ALG were deposited *in-situ* at the surface of a gold-quartz crystal sensor. Then, phage solution was purged into the chamber containing 11-layer CHI/ALG coated sensor for 30 minutes. After rinsing with DI water, the frequency was fixed. The increase in mass due to bacteriophage deposition was calculated as 1.02 $\mu g/cm^2$ (Fig. 9).

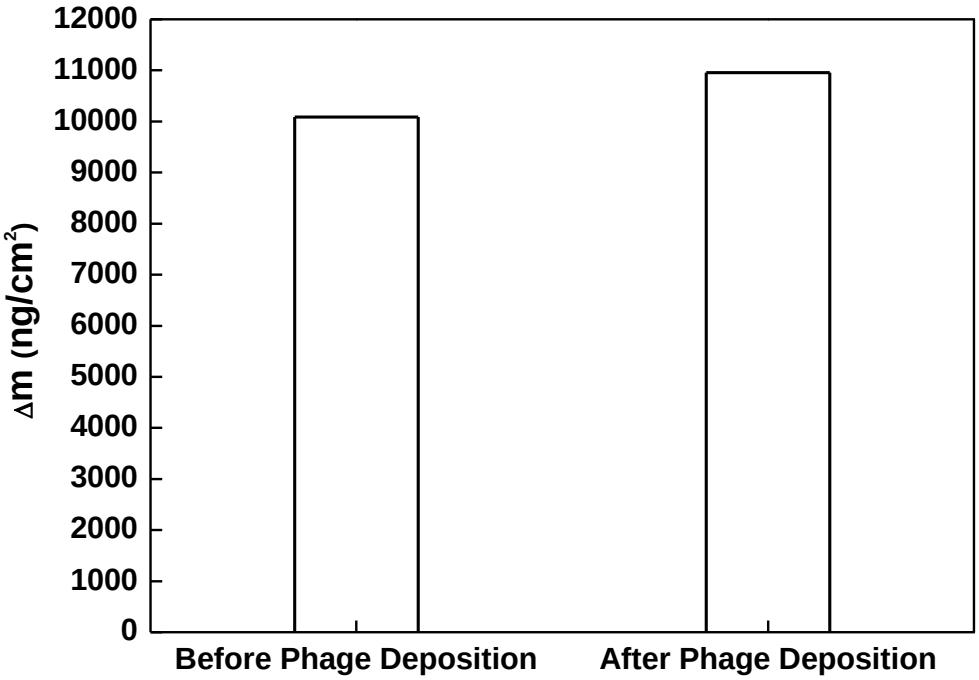

Figure 9. Mass increment upon bacteriophage loading into 11-layer CHI/ALG films.

The mass increment was calculated by using the frequency decrease due to deposition of each layer onto the substrate. However, QCM-D gives information about dissipation, too. Dissipation (damping) term corresponds to the total energy loss per oscillation cycle. In other words, dissipation can be defined as the energy dissipated per oscillation divided by the total energy of the system. The dissipation is determined from the time it takes for the oscillation to decay totally when the drive generator output is stopped. When a soft film attaches to the surface, dissipation increases because quartz crystal is deformed during the oscillation and the decay of the energy takes longer time, resulting in higher dissipation. On the other hand, if a rigid material is deposited at the crystal surface, crystal oscillates without deformation, resulting in lower dissipation [88]. Figure 10 shows the change in frequency and dissipation upon LbL deposition of CHI and ALG as well as loading of bacteriophages into multilayers. The frequency decreased during the LbL

deposition and bacteriophage loading, indicating the increase in mass on the substrate surface. On the other hand, dissipation increased as CHI and ALG were LbL-deposited since surface was coated with a soft polymeric material. However, a decrease in dissipation was observed after phage incorporation into the multilayers, pointing out that the film structure became more rigid. It was because of the bacteriophages filling the voids within the multilayers and the valleys on the surface.

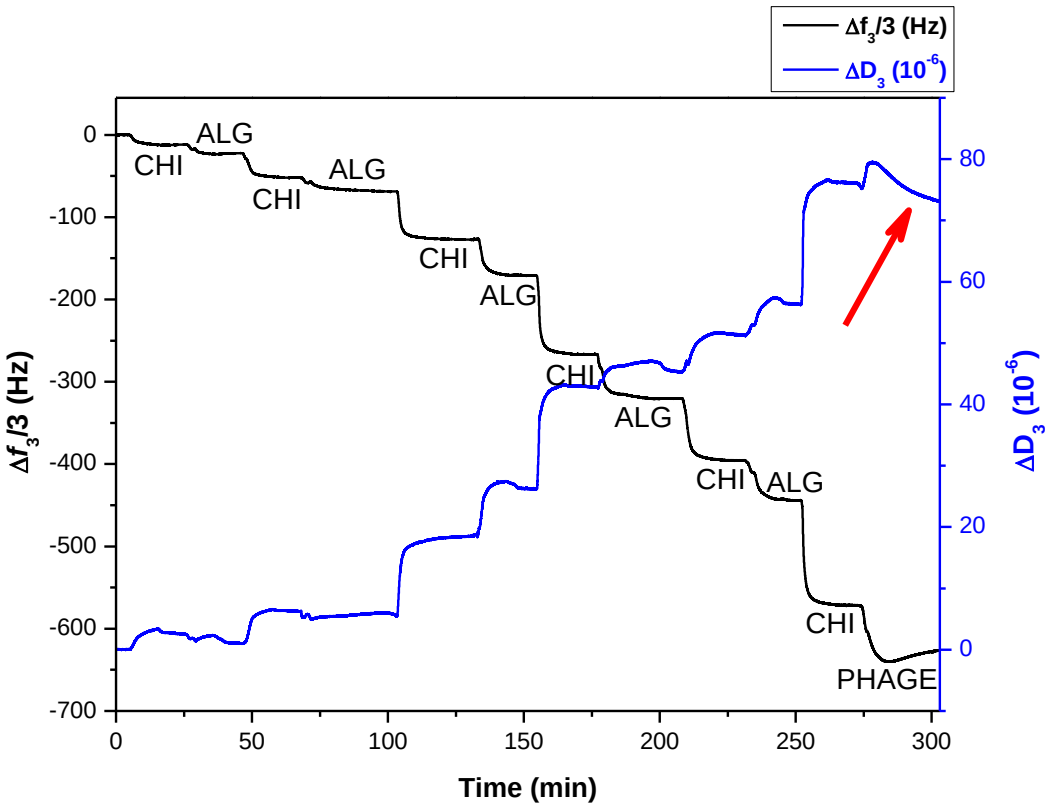

Figure 10. Evolution of the change in $\Delta f_3/n$ and ΔD_3 during LbL assembly of CHI/ALG and consequent bacteriophage loading.

3.4.2 AFM Analysis

Considering the high surface roughness of CHI/ALG multilayers (especially at high layer numbers) and the possible difficulty in visualization of bacteriophages at the surface of polymer multilayers, a preliminary study was conducted with 1-layer CHI

coated substrates which were post-loaded with bacteriophages. As seen in Figure 11, phages deposited onto 1-layer CHI could be clearly detected CHI from phase contrast (Fig.11a), height mode and topography (Fig.11b) and cross-sectional analysis (Fig.11c). Topographic images indicate that phages can be found as individual particles or phage aggregates consisting of two-three phages. Additionally, the height profile of phage deposited 1-layer CHI film clearly shows individual phages sit on and sink into the surface, since height of the phages are no larger than 4 nm. Cross-sectional analysis results indicate that there are particles with 40.9±3.5 nm average size, and this corresponds to heads of the phages according to the size analysis performed through TEM imaging of bacteriophages.

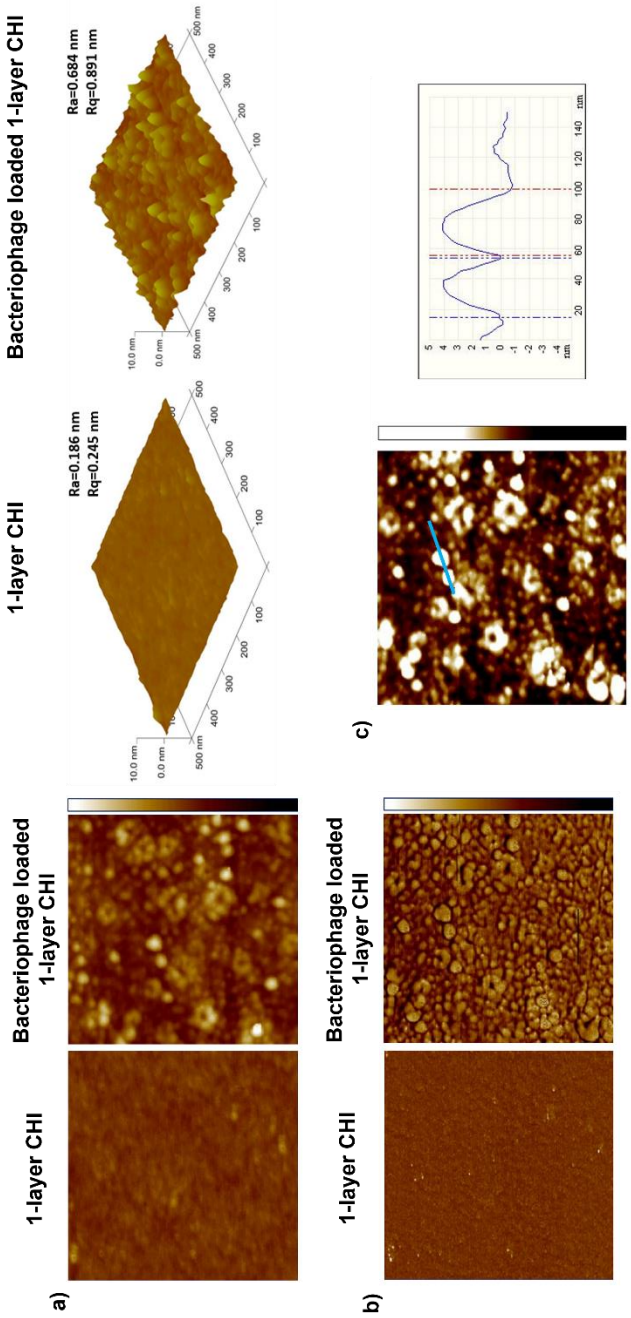

Figure 11. a) Height mode and topographic images (scan size = 500 nm × 500 nm, hmax = 10.0 nm) and roughness values (Ra & Rq) of 1-layer CHI film before and after bacteriophage loading. b) Phase contrast images (scan size = 500 nm × 500 nm, ΔΦmax = 20.0°), c) cross-sectional analysis of bacteriophage deposited 1-layer CHI film (scan size = 500 nm × 500 nm, h_{max} = 10.0 nm) and variation of height (Z) along the diagonal line marked (blue line) in the image.

AFM analysis was then conducted with 11- and 41-layer CHI/ALG films (Fig 12). The phages cannot be seen, as clear as the phage adsorbed 1-layer CHI film, when loaded into multilayers because of the high surface roughness. However, there is a significant decrease in roughness of 11- and 41-layer CHI/ALG films after phage loading. The decrease in roughness was due to the bacteriophages filling of the valleys on the surface of the film.

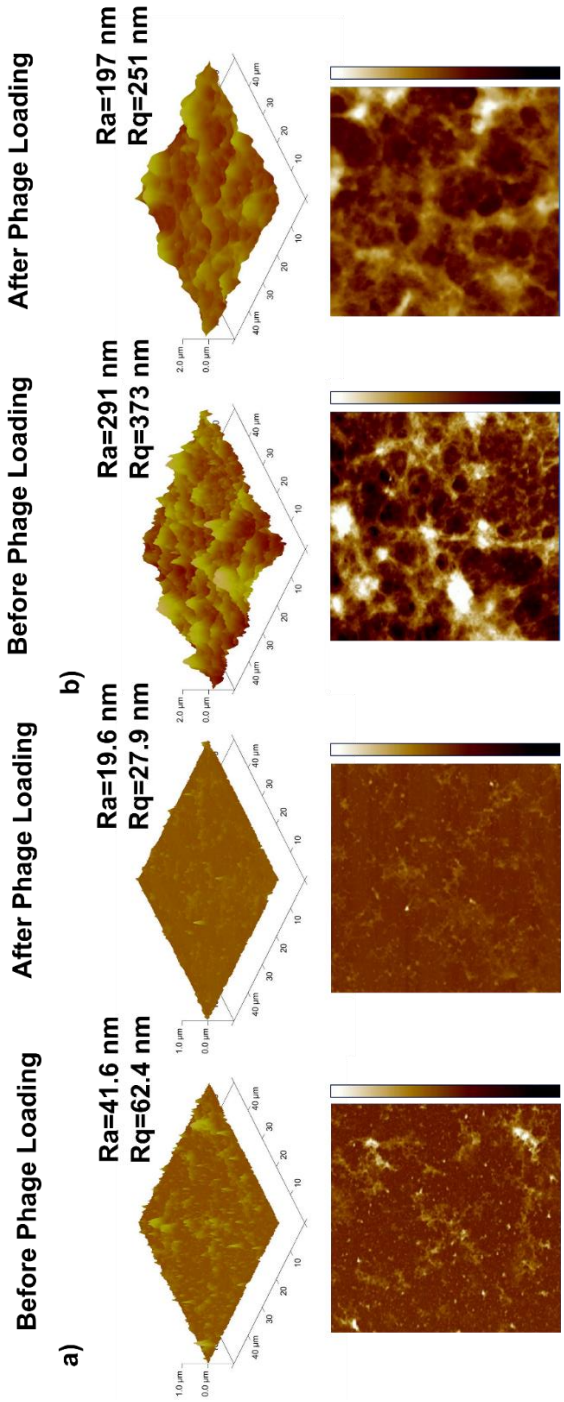

Figure 12. AFM height (left) and topography images (right) of 11-layer (a) and 41-layer (b) CHI/ALG films before and after bacteriophage loading. Different z scales in 11- and 41-layer CHI-ALG images should be noted for.

3.5 Antibacterial Effect of Phage Loaded $(CHI\text{-}ALG)_5$-CHI Multilayer Films

Disk diffusion test was applied to observe antibacterial effect of phage loaded multilayers against *Salmonella enterica* serovar Enteritidis. For this experiment, five different 11-layer coated substrates were prepared; one as negative control (only LbL coating), one positive control with CIP loaded, and three replicates of phage loaded multilayers. Bacteriophage solution pH was fixed at 7.0 before loading into multilayers. Zone formation was observed at pH 7.0 and 37 ℃, indicating the diffusion of bacteriophages from the multilayers (Fig.13). Considering that phages were loaded also at pH 7.0, the release of phages from the multilayers was correlated with the increasing temperature from 25 ℃ to 37 ℃, possibly resulting in partial loss of association among electrostatic and hydrogen bonding interactions among the layers.

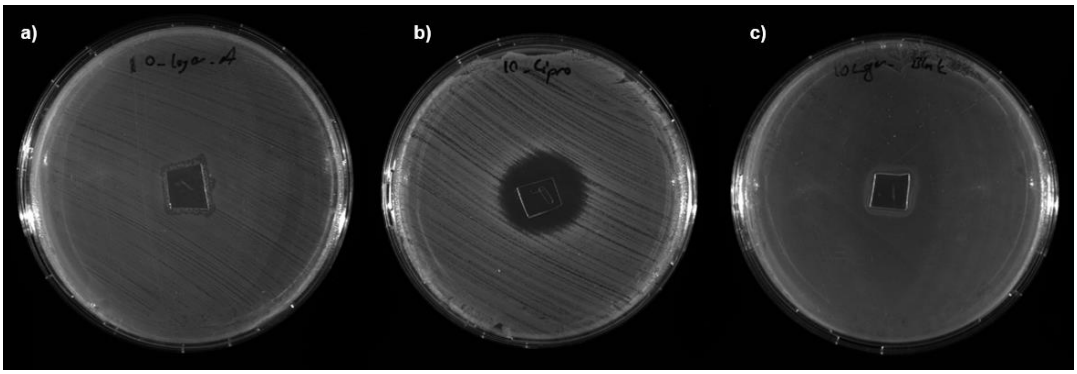

Figure 13. Disk diffusion test results of a) bacteriophage and b) CIP loaded 11-layer CHI/ALG film at pH 7.0 and 37 ℃, c) unloaded 11-layer CHI/ALG film as control substrate after 18 hours incubation.

3.6 Comparison of Number of Layers on Antibacterial Properties of $(CHI\text{-}ALG)_n$-CHI Multilayer Films

Disc-diffusion Test was performed with 1, 11, 25 and 41-layer CHI/ALG films at pH 7.0 against *Salmonella enterica* serovar Enteritidis to understand the effect of layer number on the antibacterial activity of phages. For each set having a different

layer number, there is one blank substrate which is only LbL-coated, one positive control film which is CIP loaded and three phage loaded films. It was observed that the antibacterial effect of bacteriophages was proportional to the layer number of the films (Fig.14). Indeed, this was the indication of successful bacteriophage loading into multilayers. Phages adsorbed onto 1-layer CHI coated films formed a very small zone in comparison with 11-, 25- and 41-layer films, indicating that the amount of phages adsorbed onto 1-layer CHI film was not enough to observe antibacterial activity. It must be borne in mind that surface roughness increased with increasing layer number in the film. Increasing surface roughness provided greater surface area for bacteriophage loading leading to larger zone sizes with increasing layer number.

Since, the clearest zone was observed with 41-layer films, following disc-diffusion experiments were conducted with 41-layer films in the rest of the study. Additionally average radius of zone formation was 41.0 ± 1.4 mm for positive CIP control films and 15.4 ± 1.1 mm for phage loaded $(CHI\text{-}ALG)_{20}$-CHI multilayer films. Time dependent zone formation for 41-layer films was also followed between 9^{th} and 18^{th} hours. There was no significant difference in zone size. Therefore, zone expansion with increasing time, in other words diffusion of bacteriophages, could not be observed. As bacteria grew with time, zone did not show growth in size, but became more visible due to bacterial growth on the plate.

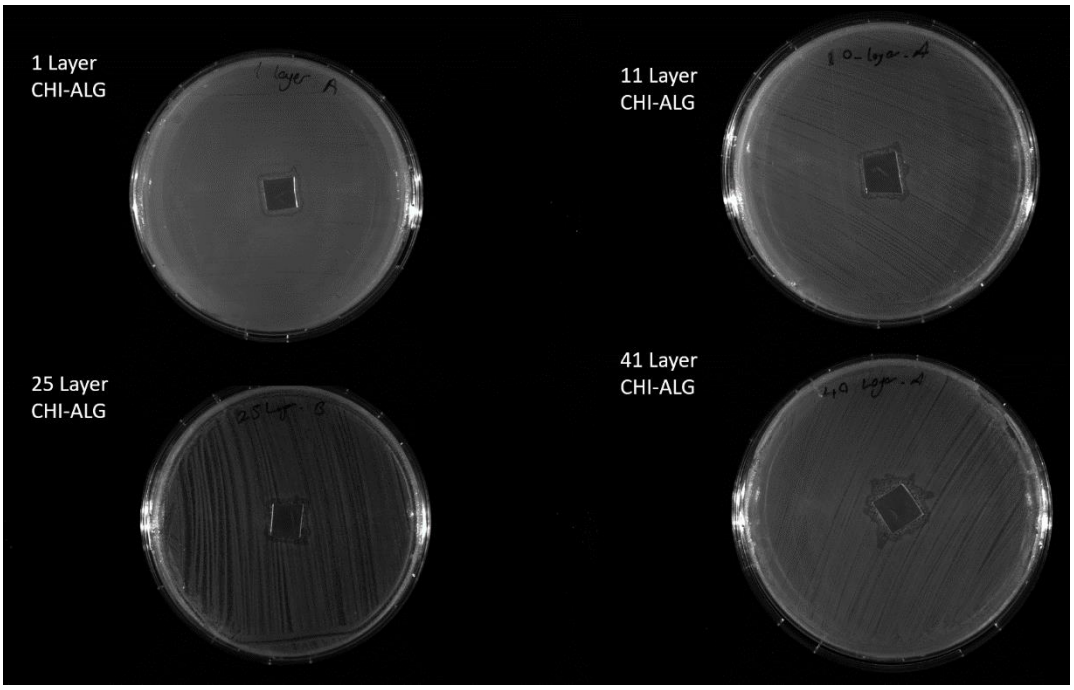

Figure 14. Disk diffusion test results of 1-, 11-, 25- and 41-layer CHI/ALG films at pH 7.0 and 37 ℃ after 18 hours incubation.

Note that the effect of pH on bacteriophage loading has also been examined. For this purpose, 5 different 11-layer CHI/ALG coated substrates were prepared also at pH 5.0. One was used as a negative control, one was loaded with CIP and used as a positive control and the other three were loaded with bacteriophages at pH 5.0 and used as replicates. There was no zone formation observed for bacteriophage loaded replicates and CIP loaded positive control. At pH 5.0, the electrostatic association between CHI and ALG was enhanced due to protonation of the amino groups of CHI. This results in more intense film structure and possibly supressed loading of bacteriophages into the multilayers. This suggests that phages were not adsorbed only at the surface of the multilayers but also incorporated within the multilayers at pH 7.0. Moreover, the roughness of CHI/ALG films might have increased at pH 7.0 due to weakening of the association between CHI and ALG. This might have provided greater surface area for phage deposition at pH 7 compared to pH 5.

3.7 Comparison of pH of Release Medium on Antibacterial Effect on (CHI-ALG)$_{20}$-CHI Multilayer Films

The antibacterial activity of phage loaded 41-layer CHI/ALG films was examined at pH 7.0 and 5.0 against *Salmonella enterica* serovar Enteritidis. Such a range was preferred because pH of meat (pork, lamb, turkey, chicken and beef) is generally between pH 5.0 and 7.0 when stored in the fridge for 10 days [89].

At pH 5.0, no clear zone formation was observed for both positive CIP control and phage loaded films (Fig. 15). At pH 5.0, the electrostatic association between CHI and ALG was enhanced due to protonation of the amino groups of CHI. This results in more intense film structure and supresses release of not only bacteriophages but also CIP although its size is much smaller than that of a bacteriophage. Additionally, since phages were negatively charged, their interaction with positively charged CHI was also expected to be greater. This causes inactivation of phages and inhibition of phage release from the surface, hence, deduced antibacterial effect.

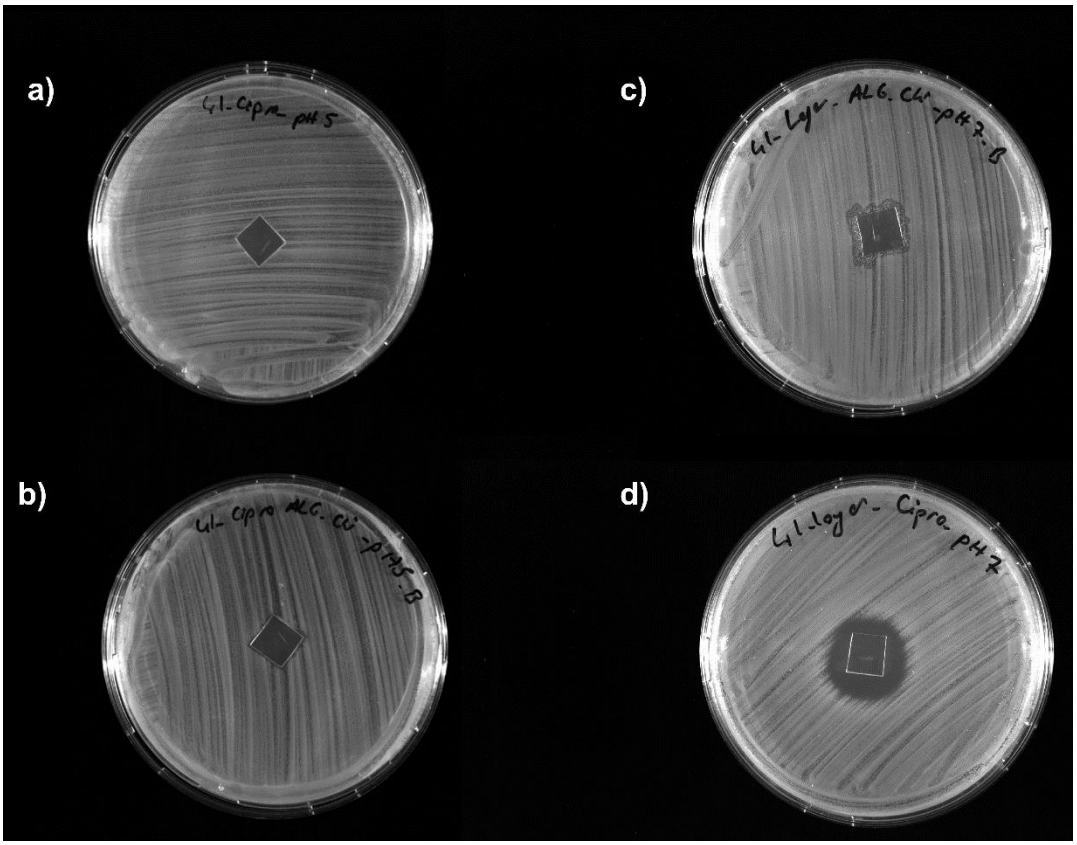

Figure 15. Disc-diffusion tests of a) CIP b) Bacteriophage loaded $(CHI\text{-}ALG)_{20}$-CHI films at pH 5.0, 37 ^{o}C; c) CIP and d) Phage loaded $(CHI\text{-}ALG)_{20}$-CHI films at pH 7.0, 37 ^{o}C.

3.8 Antibacterial Activity of CUR, THY, LA and TA Loaded $(CHI\text{-}ALG)_{20}$-CHI Multilayer Films

In this part of the study, several different antibacterial agents, i.e. CUR, THY, LA and TA, were loaded into multilayers for comparison of the antibacterial activity of the surfaces with that of phage loaded CHI/ALG films. Antibacterial activities of antibacterial agent loaded 41-layer films were tested against *Salmonella enterica* serovar Enteritidis *via* Kirby-Bauer disk diffusion method at pH 7.0 and 37^{o}C (Fig. 16). These molecules are in the category of GRAS (generally considered as safe) and can be used for food packaging applications unlike antibiotics. Antibiotics are

strongly discouraged for food safety applications because they promote evolution of multidrug resistant bacteria. Organic acids and natural molecules extracted from plant based essential oils showing antibacterial properties are considered as one of the most potent antibacterial agents for packaging applications [90,91]. Therefore, effectivity of these molecules was compared with the bacteriophages when they were encapsulated in the multilayer films. The agents are chosen from essential oils/extracts and organic acids that show antimicrobial effect. Metal ions and nanoparticles are avoided because of their potential toxicity, even in low concentrations (for example; 0.05 mg/kg of a maximum food migration of silver ion for silver zeolite [15]).

There was no zone formation observed for all the antibacterial molecules tested. It was because these natural molecules were not as effective as antibiotics and released antibacterial agents should be high in concentration to be able to observe zone formation. The concentration of the loading solutions was kept at 0.2 mg/mL for CUR, 0.5 mg/mL for THY; and 1.0 mg/mL for lactic acid and tannic acid to assure solubility of the antibacterial agents. Higher concentrations resulted in precipitation during loading process. The duration of loading was fixed at 18 hours. Even though CHI/ALG multilayers were highly porous and thick, they were still not eligible enough to encapsulate the required amount of molecules to observe any zone formation.

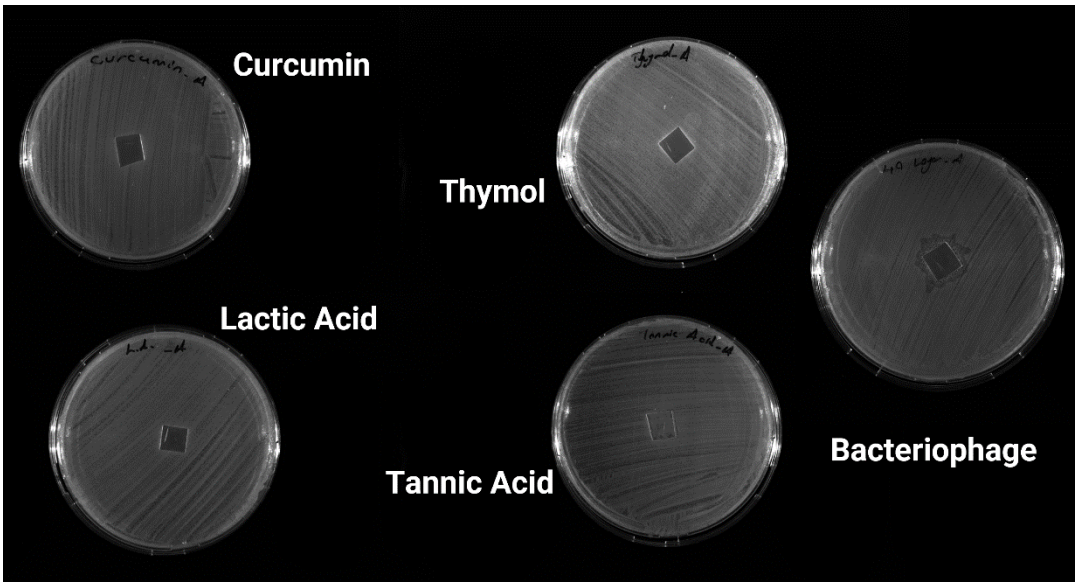

Figure 16. Disc-diffusion test of; curcumin, thymol, lactic acid, tannic acid, and bacteriophage loaded 41-layer films at pH 7.0, 37 ^{o}C after 18 hours of incubation.

CHAPTER 4

CONCLUSION

This study presented fabrication of bacteriophage incorporated CHI/ALG multilayer films for potential use in antibacterial food packaging applications. Ultrathin CHI/ALG multilayers were prepared using LbL technique. The effect of drying process during LbL assembly on the film growth profile was examined. Drying between deposition of layers was found to lead to LbL growth with a linear profile. On the other hand, drying only at the end of LbL process resulted in exponential growth of the films. This difference was correlated with the drying induced ordering of the layers at the surface. Exponential growth of multilayers was explained with the relatively weak association of CHI and ALG layers due to partial ionization of especially ALG at the film deposition pH. This resulted in a number of loops within the multilayers, leading to relatively high surface roughness. The surface roughness increased with increasing layer number, providing additional surface area for the deposition of polymer layers. The increase in surface area for deposition of polymers with increasing layer number was correlated with the exponential growth CHI and ALG.

Since, non-dried films are thicker, rougher, more porous, and more practical to produce, bacteriophage encapsulation and the following characterizations were followed using exponentially grown multilayers which were prepared without any drying process between layer depositions. The average size of bacteriophages was determined as ~200 nm through DLS analysis. TEM imaging clearly showed the head and tail parts of the phages. According to size analysis *via* TEM imaging, the head and tail parts were ~50 nm and ~100 nm in size, respectively. The size analysis obtained through DLS and TEM imaging techniques were in good agreement with each other. Characterization of phages on polymer layers was conducted through AFM imaging. Phages were adsorbed onto 1-, 11- and 41-layer CHI/ALG films. The

morphology of the phages was clearly visualized when adsorbed onto 1-layer CHI films. The cross-sectional size analysis result through AFM imaging was in good agreement with the size analysis obtained through DLS and TEM imaging techniques. Phages could not be visualized when deposited onto 11- and 41-layer films due to high surface roughness of the multilayers. However, for 11- and 41-layer films, surface roughness decreased distinctly upon loading of phages into multilayers. This was attributed to partial filling of the holes in the multilayers by the bacteriophages, resulting in a decrease in surface roughness. This was considered as an indication that bacteriophages were adsorbed on the valleys at the surface and at the same time, they filled the holes within the multilayers.

The antibacterial activity of phage loaded LbL films was investigated through Kirby-Bauer tests. Clear zones were observed when phages were deposited at pH 7.0 and Kirby Bauer tests were performed at pH 7.0. This clearly indicated release of phages from the multilayers. The zone sizes increased as the layer number increased in the films. This was attributed to larger multilayer matrix, hosting greater number of phages together with higher surface roughness which provided additional sites for phage deposition. The pH at which phages were incorporated into multilayers was also found to be critical on the antibacterial activity of the multilayers. Larger zones were obtained when phages were deposited at pH 7.0 than that at pH 5.0. This can be explained by the weaker association among CHI and ALG as the pH was increased due to deprotonation of CHI, allowing higher amount of phages being incorporated into the multilayers. The effect of pH on the antibacterial activity of the multilayers was also examined. Kirby Bauer tests were conducted at pH 5.0. Zone formation was not observed. This was possibly due to stronger association among positively charged CHI and negatively charged ALG and bacteriophages as the pH was decreased and ionization of CHI was enhanced.

Finally, antibacterial effect of an antibiotic, bacteriophages and several essential oils, extracts and organic acids were compared. Clear and perfectly round inhibition zones were not formed by bacteriophages unlike antibiotic ciprofloxacin. However, antibacterial performance of bacteriophages was found to be greater compared to

curcumin, thymol, lactic acid, and tannic acid. During this discussion, it is useful to keep in mind that antibiotics are prohibited for food packaging applications, however, phages and other mentioned molecules are not subject to such precautions.

Overall, this thesis study generated fundamental information on preparation and physicochemical characterization of ultra-thin CHI/ALG multilayer films, prepared through LbL self-assembly technique. In addition, it showed that CHI/ALG films could function as a host platform for bacteriophages. CHI and ALG are two promising natural biopolymers to reduce the negative environmental impact of non-biodegradable/recyclable materials. Bacteriophages have been drawing increasing attention as antibacterial molecules for food technology applications. Therefore, this study paves the way for phage induced coating technologies that can be applied on food packaging materials to show antibacterial effect that increase shelf life of food. The results obtained in this study may form a basis for the development of new antibacterial materials to replace the conventional packaging materials.

REFERENCES

[1] M.Y. Khalid, Z.U. Arif, Novel biopolymer-based sustainable composites for food packaging applications: A narrative review, Food Packag. Shelf Life. 33 (2022) 100892. https://doi.org/10.1016/j.fpsl.2022.100892.

[2] M.W. Ahmed, M.A. Haque, M. Mohibbullah, M.S.I. Khan, M.A. Islam, M.H.T. Mondal, R. Ahmmed, A review on active packaging for quality and safety of foods: Current trends, applications, prospects and challenges, Food Packag. Shelf Life. 33 (2022) 100913. https://doi.org/10.1016/j.fpsl.2022.100913.

[3] J. Wang, M. Euring, K. Ostendorf, K. Zhang, Biobased materials for food packaging, J. Bioresour. Bioprod. 7 (2022) 1–13. https://doi.org/10.1016/j.jobab.2021.11.004.

[4] M.L. Rooney, Overview of active food packaging BT - Active Food Packaging, in: M.L. Rooney (Ed.), Springer US, Boston, MA, 1995: pp. 1–37. https://doi.org/10.1007/978-1-4615-2175-4_1.

[5] J. Sneller, Modified-atmosphere Packaging of Fish and Fish Products, Mod. Plast. Int. 16 (1986) 58–59.

[6] G.L. Robertson, F. Group, Food Packaging: Principles and Practice, n.d.

[7] J.P. Kerry, M.N.O. Grady, S.A. Hogan, Meat Past , current and potential utilisation of active and intelligent packaging systems for meat and muscle-based products : A review, 74 (2006) 113–130. https://doi.org/10.1016/j.meatsci.2006.04.024.

[8] N.H. Azman, W.M. Khairul, N.M. Sarbon, A comprehensive review on biocompatible film sensor containing natural extract: Active/intelligent food packaging, Food Control. 141 (2022) 109189. https://doi.org/10.1016/j.foodcont.2022.109189.

[9] A. Mousavi, S. Mohammad, B. Hashemi, S. Limbo, Food and Bioproducts Processing Antimicrobial agents and packaging systems in antimicrobial active food packaging : An overview of approaches and interactions, Food Bioprod. Process. 111 (2018) 1–19. https://doi.org/10.1016/j.fbp.2018.05.001.

[10] A. Moeini, N. Germann, M. Malinconico, G. Santagata, Formulation of secondary compounds as additives of biopolymer-based food packaging: A review, Trends Food Sci. Technol. 114 (2021) 342–354. https://doi.org/10.1016/j.tifs.2021.05.040.

[11] V. Siracusa, P. Rocculi, S. Romani, M.D. Rosa, Biodegradable polymers for food packaging: a review, Trends Food Sci. Technol. 19 (2008) 634–643. https://doi.org/10.1016/j.tifs.2008.07.003.

[12] H. Wang, X. Gong, Y. Miao, X. Guo, C. Liu, Y.Y. Fan, J. Zhang, B. Niu, W. Li, Preparation and Characterization of Multilayer Films Composed of Chitosan, Sodium Alginate and Carboxymethyl Chitosan-ZnO Nanoparticles, Food Chem. 283 (2019) 397–403. https://doi.org/10.1016/j.foodchem.2019.01.022.

[13] Y. Zhang, Q. Liu, C. Rempel, Processing and Characteristics of Canola Protein- based Biodegradable Packaging : A Review, 8398 (2016). https://doi.org/10.1080/10408398.2016.1193463.

[14] H. Arnon-Rips, E. Poverenov, Improving food products' Quality and Storability by Using Layer by Layer Edible Coatings, Trends Food Sci. Technol. 75 (2018) 81–92. https://doi.org/10.1016/j.tifs.2018.03.003.

[15] S. Quintavalla, L. Vicini, Antimicrobial Food Fackaging in Meat Industry, 62 (2002) 373–380.

[16] C. Bilbao-Sainz, B. Sen Chiou, K. Punotai, D. Olson, T. Williams, D. Wood, V. Rodov, E. Poverenov, T. McHugh, Layer-by-Layer Alginate and Fungal Chitosan Based Edible Coatings Applied to Fruit Bars, J. Food Sci. 83 (2018)

1880–1887. https://doi.org/10.1111/1750-3841.14186.

[17] A.R. Shirvan, M. Shakeri, A. Bashari, Recent Advances in Application of Chitosan and its Derivatives in Functional Finishing of Textiles, Elsevier Ltd., 2019. https://doi.org/10.1016/B978-0-08-102491-1.00005-8.

[18] J.C. Roy, F. Salaün, S. Giraud, A. Ferri, G. Chen, J. Guan, Solubility of Chitin: Solvents, Solution Behaviors and Their Related Mechanisms, in: Zhenbo Xu (Ed.), Solubility of Polysaccharides, InTech, Rijeka, 2017. https://doi.org/10.5772/intechopen.71385.

[19] Y. Cho, J. Jang, C.R. Park, S. Ko, Preparation and Solubility in Acid and Water of Partially Deacetylated Chitins, (2000) 609–614.

[20] J. Lizardi-mendoza, W.M.A. Monal, F.M.G. Valencia, Chemical Characteristics and Functional Properties of Chitosan, Elsevier Inc., 2016. https://doi.org/10.1016/B978-0-12-802735-6/00001-X.

[21] H. Maros, S. Juniar, Alginates: Versatile Polymers in Biomedical Applications and Therapeutics, 2016.

[22] J.J. Chuang, Y.Y. Huang, S.H. Lo, T.F. Hsu, W.Y. Huang, S.L. Huang, Y.S. Lin, Effects of pH on the Shape of Alginate Particles and Its Release Behavior, Int. J. Polym. Sci. 2017 (2017). https://doi.org/10.1155/2017/3902704.

[23] K. Varaprasad, T. Jayaramudu, V. Kanikireddy, C. Toro, E.R. Sadiku, Alginate-based composite materials for wound dressing application:A mini review, Carbohydr. Polym. 236 (2020) 116025. https://doi.org/10.1016/j.carbpol.2020.116025.

[24] T.S. Parreidt, K. Müller, M. Schmid, Alginate-based edible films and coatings for food packaging applications, Foods. 7 (2018) 1–38. https://doi.org/10.3390/foods7100170.

[25] S.T. Abedon, The bacteriophages, 1969. https://doi.org/10.1016/0002-9343(69)90010-2.

[26] X. Wittebole, S. De Roock, S.M. Opal, A historical overview of bacteriophage therapy as an alternative to antibiotics for the treatment of bacterial pathogens, Virulence. 5 (2014) 226–235. https://doi.org/10.4161/viru.25991.

[27] Z. Golkar, O. Bagasra, D. Gene Pace, Bacteriophage therapy: A potential solution for the antibiotic resistance crisis, J. Infect. Dev. Ctries. 8 (2014) 129–136. https://doi.org/10.3855/jidc.3573.

[28] B. Burrowes, D.R. Harper, J. Anderson, M. McConville, M.C. Enright, Bacteriophage therapy: Potential uses in the control of antibiotic-resistant pathogens, Expert Rev. Anti. Infect. Ther. 9 (2011) 775–785. https://doi.org/10.1586/eri.11.90.

[29] S.M. Sillankorva, H. Oliveira, J. Azeredo, Bacteriophages and their role in food safety, Int. J. Microbiol. 2012 (2012). https://doi.org/10.1155/2012/863945.

[30] L. Endersen, A. Coffey, The use of bacteriophages for food safety, Curr. Opin. Food Sci. 36 (2020) 1–8. https://doi.org/10.1016/j.cofs.2020.10.006.

[31] T.J. Török, R. V. Tauxe, R.P. Wise, J.R. Livengood, R. Sokolow, S. Mauvais, K.A. Birkness, M.R. Skeels, J.M. Horan, L.R. Foster, A large community outbreak of salmonellosis caused by intentional contamination of restaurant salad bars, Jama. 278 (1997) 389–395. https://doi.org/10.1001/jama.278.5.389.

[32] R.J. Atterbury, M.A.P. Van Bergen, F. Ortiz, M.A. Lovell, J.A. Harris, A. De Boer, J.A. Wagenaar, V.M. Allen, P.A. Barrow, A.P.P.L.E.N.M. Icrobiol, Bacteriophage Therapy To Reduce Salmonella Colonization of Broiler Chickens , 73 (2007) 4543–4549. https://doi.org/10.1128/AEM.00049-07.

[33] R. Modi, Y. Hirvi, A. Hill, Effect of Phage on Survival of Salmonella Enteritidis during Manufacture and Storage of Cheddar Cheese Made from Raw and Pasteurized Milk, 64 (2001) 927–933.

[34] J.M. Whichard, N. Sriranganathan, F.W. Pierson, Suppression of Salmonella Growth by Wild-Type and Large-Plaque Variants of Bacteriophage Felix O1 in Liquid, 66 (2003) 220–225.

[35] C. Zhang, C. Li, J. Aliakbarlu, H. Cui, L. Lin, Typical application of electrostatic layer-by-layer self-assembly technology in food safety assurance, Trends Food Sci. Technol. 129 (2022) 88–97. https://doi.org/10.1016/j.tifs.2022.09.006.

[36] R. K. Iler, Multilayers of colloidal particles, J. Colloid Interface Sci. 21 (1966) 569–594.

[37] G. Decher, J.D. Hong, J. Schmitt, Buildup of ultrathin multilayer films by a self-assembly process: III. Consecutively alternating adsorption of anionic and cationic polyelectrolytes on charged surfaces, Thin Solid Films. 210–211 (1992) 831–835. https://doi.org/10.1016/0040-6090(92)90417-A.

[38] G. Decher, J. Hong, J. Gutenberg-universitt, Gero Decher* and Jong-Dal Hong Institut fur Physikalische Chemie; Johannes Gutenberg-Universitt Welder Weg 11; D-6500 Maim; Fed. Rep. of Germany AbstraG, 327 (1991) 321–327.

[39] Buildup of Ultrathin Multilayer Films by a Self-Assembly Process: 11. Consecutive Adsorption of Anionic and Cationic Bipolar Amphiphiles and Polyelectrolytes on Charged Surfaces, Ber. Bunsetlges. Phys. Chem. Y5. (1991).

[40] G. Decher, J. Schmitt, Fine-Tuning of the film thickness of ultrathin multilayer films composed of consecutively alternating layers of anionic and cationic polyelectrolytes, Trends Colloid Interface Sci. VI. 164 (2007) 160–164. https://doi.org/10.1007/bfb0116302.

[41] A. Sarode, A. Annapragada, J. Guo, S. Mitragotri, Layered self-assemblies for controlled drug delivery: A translational overview, Biomaterials. 242 (2020) 119929. https://doi.org/10.1016/j.biomaterials.2020.119929.

[42] E. Poverenov, S. Danino, B. Horev, R. Granit, Y. Vinokur, V. Rodov, Layer-by-Layer Electrostatic Deposition of Edible Coating on Fresh Cut Melon Model: Anticipated and Unexpected Effects of Alginate-Chitosan Combination, Food Bioprocess Technol. 7 (2014) 1424–1432. https://doi.org/10.1007/s11947-013-1134-4.

[43] P. Wang, C. Zhang, Y. Zou, Y. Li, H. Zhang, Immobilization of lysozyme on layer-by-layer self-assembled electrospun films: Characterization and antibacterial activity in milk, Food Hydrocoll. 113 (2021) 106468. https://doi.org/10.1016/j.foodhyd.2020.106468.

[44] J.R. Lakkakula, P. Gujarathi, P. Pansare, S. Tripathi, A comprehensive review on alginate-based delivery systems for the delivery of chemotherapeutic agent: Doxorubicin, Carbohydr. Polym. 259 (2021) 117696. https://doi.org/10.1016/j.carbpol.2021.117696.

[45] W. Song, Q. He, H. Möhwald, Y. Yang, J. Li, Smart polyelectrolyte microcapsules as carriers for water-soluble small molecular drug, J. Control. Release. 139 (2009) 160–166. https://doi.org/10.1016/j.jconrel.2009.06.010.

[46] P.K. Deshmukh, K.P. Ramani, S.S. Singh, A.R. Tekade, V.K. Chatap, G.B. Patil, S.B. Bari, Stimuli-sensitive layer-by-layer (LbL) self-assembly systems: Targeting and biosensory applications, J. Control. Release. 166 (2013) 294–306. https://doi.org/10.1016/j.jconrel.2012.12.033.

[47] R.M. Iost, F.N. Crespilho, Layer-by-layer self-assembly and electrochemistry: Applications in biosensing and bioelectronics, Biosens. Bioelectron. 31 (2012) 1–10. https://doi.org/10.1016/j.bios.2011.10.040.

[48] F.N. Crespilho, M. Emilia Ghica, M. Florescu, F.C. Nart, O.N. Oliveira, C.M.A. Brett, A strategy for enzyme immobilization on layer-by-layer dendrimer-gold nanoparticle electrocatalytic membrane incorporating redox mediator, Electrochem. Commun. 8 (2006) 1665–1670. https://doi.org/10.1016/j.elecom.2006.07.032.

[49] C. Wang, M.J. Park, H. Yu, H. Matsuyama, E. Drioli, H.K. Shon, Recent advances of nanocomposite membranes using layer-by-layer assembly, J. Memb. Sci. 661 (2022) 120926. https://doi.org/10.1016/j.memsci.2022.120926.

[50] T. Hu, M. Zhang, Z. Wang, K. Chen, X. Li, Z. Ni, Layer-by-layer self-assembly of MoS2/PDDA hybrid film in microfluidic chips for ultrasensitive electrochemical immunosensing of alpha-fetoprotein, Microchem. J. 158 (2020) 105209. https://doi.org/10.1016/j.microc.2020.105209.

[51] Y. Hu, H. Zhao, M. Tan, J. Liu, X. Shu, M. Zhang, S. Liu, Q. Ran, H. Li, X. Liu, Synthesis of α-LiFeO2/Graphene nanocomposite via layer by layer self-assembly strategy for lithium-ion batteries with excellent electrochemical performance, J. Mater. Sci. Technol. 55 (2020) 173–181. https://doi.org/10.1016/j.jmst.2019.04.044.

[52] J. Borges, J.F. Mano, Molecular interactions driving the layer-by-layer assembly of multilayers, Chem. Rev. 114 (2014) 8883–8942. https://doi.org/10.1021/cr400531v.

[53] I.S. Elizarova, P.F. Luckham, Layer-by-layer adsorption: Factors affecting the choice of substrates and polymers, Adv. Colloid Interface Sci. 262 (2018) 1–20. https://doi.org/10.1016/j.cis.2018.11.003.

[54] P. Shende, A. Patil, B. Prabhakar, Layer-by-layer technique for enhancing physicochemical properties of actives, J. Drug Deliv. Sci. Technol. 56 (2020) 101519. https://doi.org/10.1016/j.jddst.2020.101519.

[55] P. Sher, C.A. Custódio, J.F. Mano, Layer-by-layer technique for producing porous nanostructured 3D constructs using moldable freeform assembly of spherical templates, Small. 6 (2010) 2644–2648. https://doi.org/10.1002/smll.201001066.

[56] S. Lee, J. Hong, C.H. Kim, K. Kim, J.P. Koo, K. Lee, Layer-by-Layer Deposited Multilayer Assemblies of Ionene-Type Polyelectrolytes Based on

the Spin-Coating Method, (2001) 5358–5360.

[57] T. Aradi, V. Hornok, I. Dékány, Layered double hydroxides for ultrathin hybrid film preparation using layer-by-layer and spin coating methods, Colloids Surfaces A Physicochem. Eng. Asp. 319 (2008) 116–121. https://doi.org/10.1016/j.colsurfa.2007.06.049.

[58] S. Kharlampieva, Eugenia Kozlovskaya, Veronica Sukhisvili, Layer-by-Layer Hydrogen-Bonded Polymer Films From Fundamentals to Applications, Adv. Mater., 21 (2009) .

[59] L. Wang, Z. Wang, X. Zhang, J. Shen, L. Chi, H. Fuchs, A new approach for the fabrication of an alternating multilayer film of poly(4-vinylpyridine) and poly(acrylic acid) based on hydrogen bonding, Macromol. Rapid Commun. 18 (1997) 509–514. https://doi.org/10.1002/marc.1997.030180609.

[60] J.H. Cheung, W.B. Stockton, M.F. Rubner, Molecular-level processing of conjugated polymers. 3. Layer-by-layer manipulation of polyaniline via electrostatic interactions, Macromolecules. 30 (1997) 2712–2716. https://doi.org/10.1021/ma970047d.

[61] S.A. Sukhishvili, S. Granick, Layered, erasable polymer multilayers formed by hydrogen-bonded sequential self-assembly, Macromolecules. 35 (2002) 301–310. https://doi.org/10.1021/ma011346c.

[62] G. Liu, J. Zhao, Q. Sun, G. Zhang, Role of chain interpenetration in layer-by-layer deposition of polyelectrolytes, J. Phys. Chem. B. 112 (2008) 3333–3338. https://doi.org/10.1021/jp710600f.

[63] D. Yoo, S.S. Shiratori, M.F. Rubner, Controlling bilayer composition and surface wettability of sequentially adsorbed multilayers of weak polyelectrolytes, Macromolecules. 31 (1998) 4309–4318. https://doi.org/10.1021/ma9800360.

[64] W. Yuan, H. Dong, C.M. Li, X. Cui, L. Yu, Z. Lu, Q. Zhou, pH-controlled

construction of chitosan/alginate multilayer film: Characterization and application for antibody immobilization, Langmuir. 23 (2007) 13046–13052. https://doi.org/10.1021/la702774a.

[65] T.B. Taketa, D.M. Dos Santos, A. Fiamingo, J.M. Vaz, M.M. Beppu, S.P. Campana-Filho, R.E. Cohen, M.F. Rubner, Investigation of the Internal Chemical Composition of Chitosan-Based LbL Films by Depth-Profiling X-ray Photoelectron Spectroscopy (XPS) Analysis, Langmuir. 34 (2018) 1429–1440. https://doi.org/10.1021/acs.langmuir.7b04104.

[66] H.L. Tan, M.J. McMurdo, G. Pan, P.G. Van Patten, Temperature Dependence of Polyelectrolyte Multilayer Assembly, Langmuir. 19 (2003) 9311–9314. https://doi.org/10.1021/la035094f.

[67] J. Ma, S. Yang, Y. Li, X. Xu, J. Xu, Effect of Temperature on the Build-up and Post Hydrothermal Processing of Hydrogen-bonded PVPON/PAA Film, Soft Matter. 7 (2011) 9435–9443. https://doi.org/10.1039/c1sm05587a.

[68] A.S. Vikulina, Y.G. Anissimov, P. Singh, V.Z. Prokopovic, K. Uhlig, M.S. Jaeger, R. Von Klitzing, C. Duschl, D. Volodkin, Temperature Effect on the Build-up of Exponentially Growing Polyelectrolyte Multilayers: An Exponential-to-linear Transition Point, (2016) 9–14. https://doi.org/10.1039/c6cp00345a.

[69] R. V. Klitzing, Internal Structure of Polyelectrolyte Multilayer Assemblies, Phys. Chem. Chem. Phys. 8 (2006) 5012–5033. https://doi.org/10.1039/b607760a.

[70] A. Fery, B. Schöler, T. Cassagneau, F. Caruso Nanoporous Thin Films Formed by Salt-Induced Structural Changes in Multilayers of Poly(acrylic acid) and Poly(allylamine), *Langmuir* 2001, 17, 13, 3779-3783.

[71] H. Lv, Z. Chen, X. Yang, L. Cen, X. Zhang, P. Gao, Layer-by-layer self-assembly of minocycline-loaded chitosan/alginate multilayer on titanium substrates to inhibit biofilm formation, J. Dent. 42 (2014) 1464–1472.

https://doi.org/10.1016/j.jdent.2014.06.003.

[72] J. Zhou, G. Romero, E. Rojas, L. Ma, S. Moya, C. Gao, Layer by layer chitosan/alginate coatings on poly(lactide-co-glycolide) nanoparticles for antifouling protection and Folic acid binding to achieve selective cell targeting, J. Colloid Interface Sci. 345 (2010) 241–247. https://doi.org/10.1016/j.jcis.2010.02.004.

[73] F. Chai, L. Sun, X. He, J. Li, Y. Liu, F. Xiong, L. Ge, T.J. Webster, C. Zheng, Doxorubicin-loaded poly (Lactic-co-glycolic acid) nanoparticles coated with chitosan/alginate by layer by layer technology for antitumor applications, Int. J. Nanomedicine. 12 (2017) 1791–1802. https://doi.org/10.2147/IJN.S130404.

[74] J.H. Kim, W. sung Hong, S.W. Oh, Effect of layer-by-layer antimicrobial edible coating of alginate and chitosan with grapefruit seed extract for shelf-life extension of shrimp (Litopenaeus vannamei) stored at 4 °C, Int. J. Biol. Macromol. 120 (2018) 1468–1473. https://doi.org/10.1016/j.ijbiomac.2018.09.160.

[75] H. Cui, L. Yuan, L. Lin, Novel chitosan film embedded with liposome-encapsulated phage for biocontrol of Escherichia coli O157:H7 in beef, Carbohydr. Polym. 177 (2017) 156–164. https://doi.org/10.1016/j.carbpol.2017.08.137.

[76] M. Müller, B. Urban, G.K. Mannala, V. Alt, Poly(ethyleneimine)/Poly(acrylic acid) Multilayer Coatings with Peripherally Bound Staphylococcus aureus Bacteriophages Have Antibacterial Properties, ACS Appl. Polym. Mater. 3 (2021) 6230–6237. https://doi.org/10.1021/acsapm.1c01057.

[77] G. Francius, M. Cervulle, E. Clément, X. Bellanger, S. Ekrami, C. Gantzer, J.F.L. Duval, Impacts of Mechanical Stiffness of Bacteriophage-Loaded Hydrogels on Their Antibacterial Activity, ACS Appl. Bio Mater. 4 (2021) 2614–2627. https://doi.org/10.1021/acsabm.0c01595.

[78] M. Güzel, An Alternative Way for Reduction of Salmonella in Poultry Products: Bacteriophages, Middle East Technical University, 2022.

[79] S. Acar, E. Bulut, B. Durul, I. Uner, M. Kur, M.D. Avsaroglu, H.A. Kirmaci, Y.O. Tel, F.Y. Zeyrek, Y. Soyer, Phenotyping and genetic characterization of Salmonella enterica isolates from Turkey revealing arise of different features specific to geography, Int. J. Food Microbiol. 241 (2017) 98–107. https://doi.org/10.1016/j.ijfoodmicro.2016.09.031.

[80] J. Hudzicki, Kirby-Bauer Disk Diffusion Susceptibility Test Protocol Author Information, Am. Soc. Microbiol. (2012) 1–13. https://www.asm.org/Protocols/Kirby-Bauer-Disk-Diffusion-Susceptibility-Test-Pro.

[81] G. Sauerbrey, Verwendung von Schwingquarzen zur Wägung dünner Schichten und zur Mikrowägung, Zeitschrift Für Phys. 155 (1959) 206–222. https://doi.org/10.1007/BF01337937.

[82] Q.Z. Wang, X.G. Chen, N. Liu, S.X. Wang, C.S. Liu, X.H. Meng, C.G. Liu, Protonation constants of chitosan with different molecular weight and degree of deacetylation, Carbohydr. Polym. 65 (2006) 194–201. https://doi.org/10.1016/j.carbpol.2006.01.001.

[83] M. Gierszewska, J. Ostrowska-Czubenko, E. Chrzanowska, pH-responsive chitosan/alginate polyelectrolyte complex membranes reinforced by tripolyphosphate, Eur. Polym. J. 101 (2018) 282–290. https://doi.org/10.1016/j.eurpolymj.2018.02.031.

[84] J.A.W. J.N. Hilfiker, elipsoğu, in: R.D. Guenther (Ed.), Instrum. | Ellipsom., Elsevier, 2005: pp. 297–307. https://doi.org/https://doi.org/10.1016/B0-12-369395-0/00833-2.

[85] S.S. Shiratori, M.F. Rubner, pH-dependent thickness behavior of sequentially adsorbed layers of weak polyelectrolytes, Macromolecules. 33 (2000) 4213–4219. https://doi.org/10.1021/ma991645q.

[86] E. Le Bihan-Duval, N. Millet, H. Remignon, Broiler meat quality: Effect of selection for increased carcass quality and estimates of genetic parameters, Poult. Sci. 78 (1999) 822–826. https://doi.org/10.1093/ps/78.6.822.

[87] S. Islam, M.A.R. Bhuiyan, M.N. Islam, Chitin and Chitosan: Structure, Properties and Applications in Biomedical Engineering, J. Polym. Environ. 25 (2017) 854–866. https://doi.org/10.1007/s10924-016-0865-5.

[88] J. Huang, S. Zajforoushan Moghaddam, E. Thormann, Structural Investigation of a Self-Cross-Linked Chitosan/Alginate Dialdehyde Multilayered Film with in Situ QCM-D and Spectroscopic Ellipsometry, ACS Omega. 4 (2019) 2019–2029. https://doi.org/10.1021/acsomega.8b03145.

[89] M. Triki, A.M. Herrero, F. Jiménez-Colmenero, C. Ruiz-Capillas, Quality assessment of fresh meat from several species based on free amino acid and biogenic amine contents during chilled storage, Foods. 7 (2018). https://doi.org/10.3390/foods7090132.

[90] Y.X. Seow, C.R. Yeo, H.L. Chung, H.G. Yuk, Plant Essential Oils as Active Antimicrobial Agents, Crit. Rev. Food Sci. Nutr. 54 (2014) 625–644. https://doi.org/10.1080/10408398.2011.599504.

[91] M.M. Theron, J.F.R. Lues, Organic acids and meat preservation: A review, Food Rev. Int. 23 (2007) 141–158. https://doi.org/10.1080/87559120701224964.